Oregon State University
College of Engineering

RUTGERS

Solution-based & Printable Functional Materials for Smart Fabrics

Zhongwei Gao, Shujie Li, Yujuan He, Chih-hung (Alex) Chang
Hyun-Jun Hwang, Rajiv Malhotra
School of Chemical, Biological and Environmental Engineering
Oregon State University, Corvallis, Oregon
Mechanical and Aerospace Engineering
Rutgers University

Smart Fabrics

Turn Signal Bike Jacket
Leah Buechley's Turn Signal Bike Jacket made with her Lilypad Arduino.

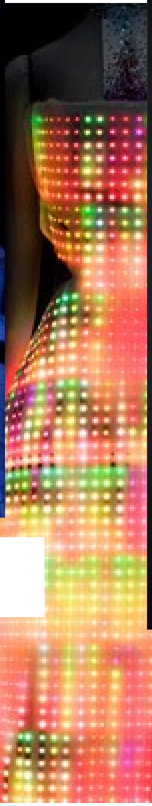

Cute Circuits

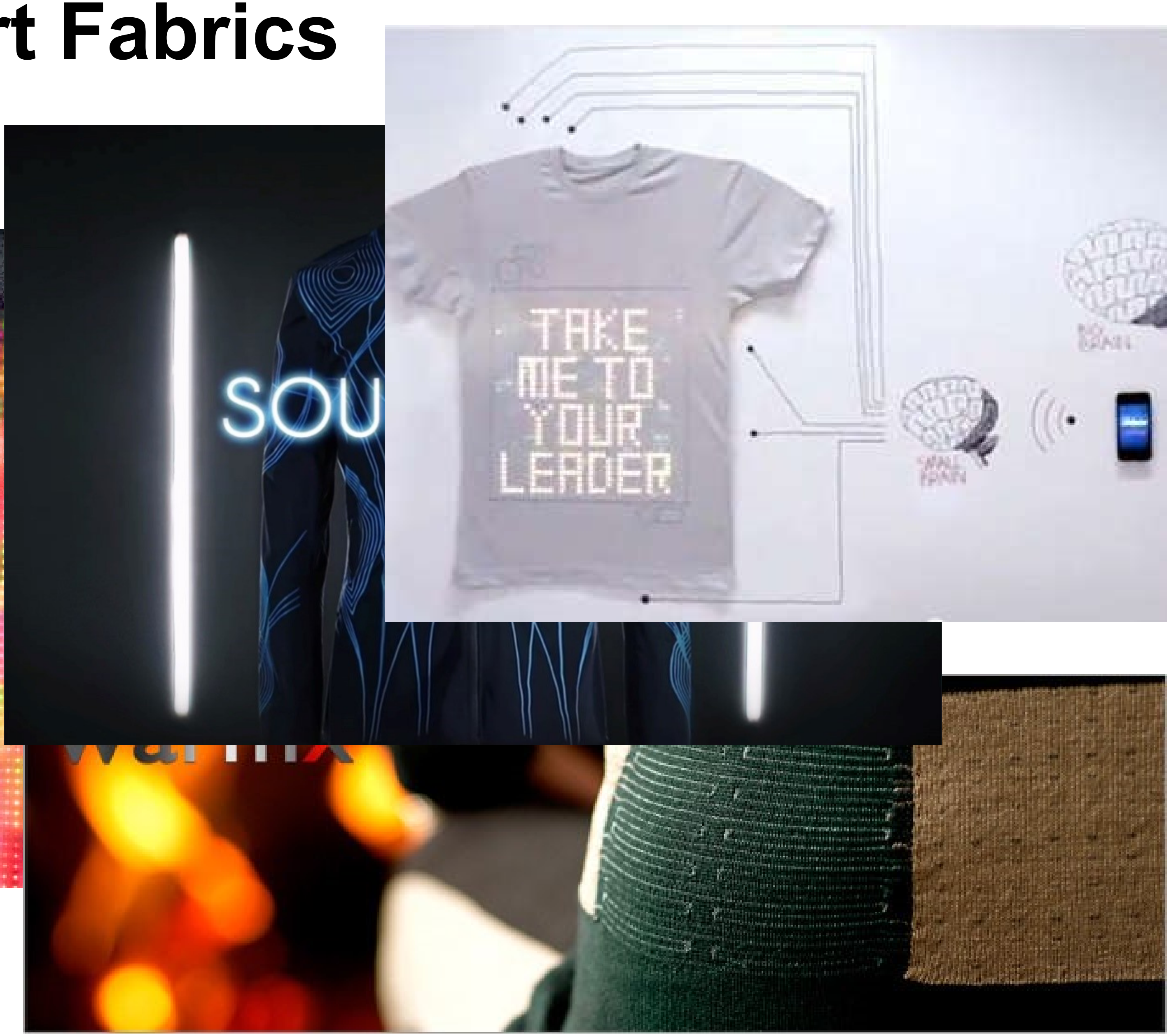

How to Make it?

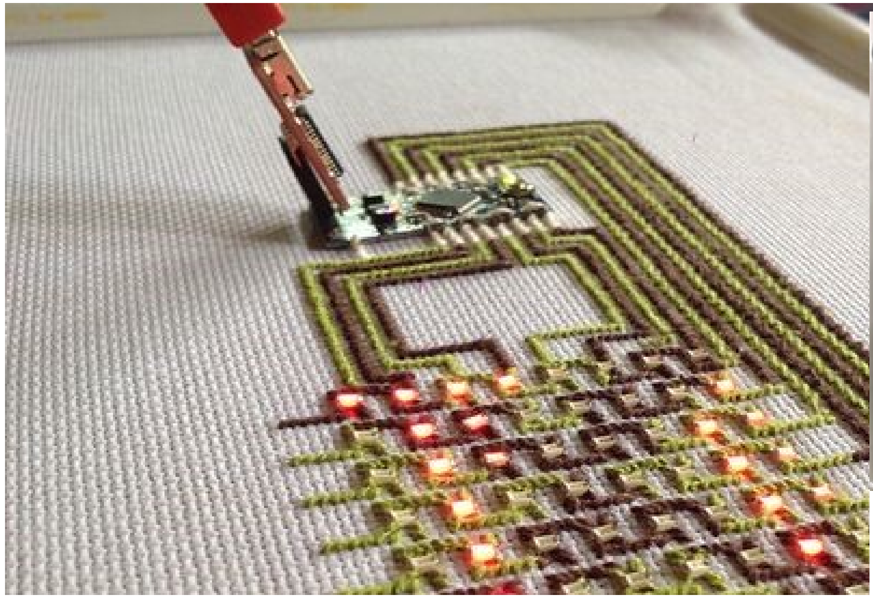

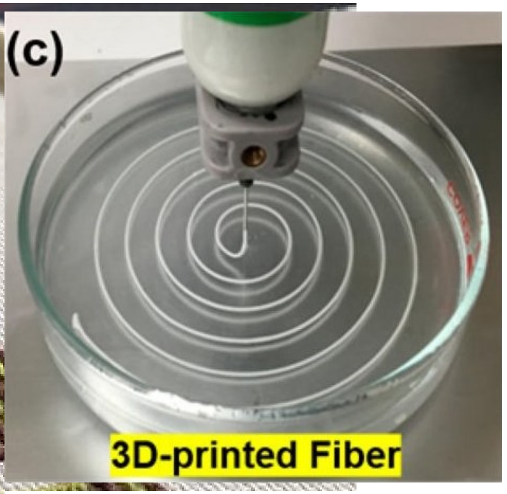

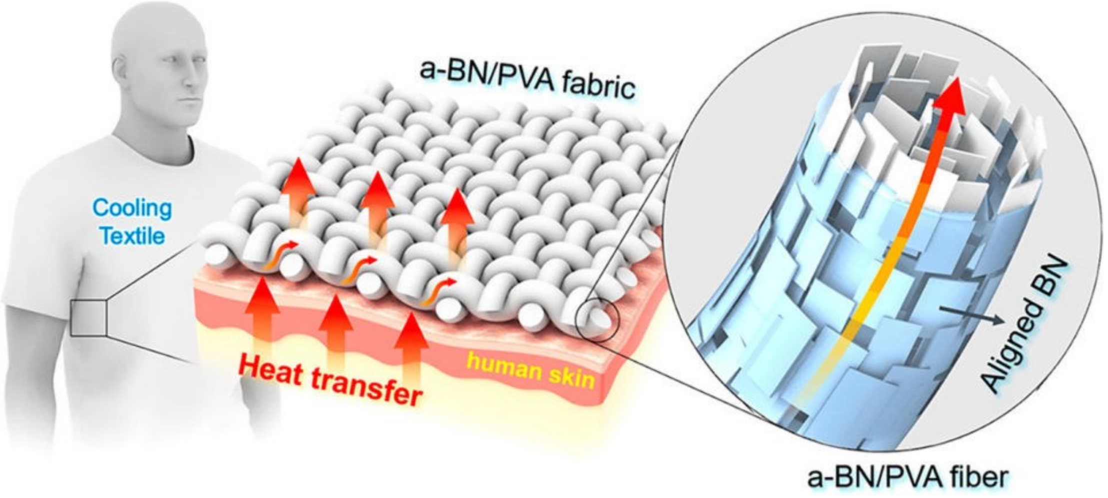

Niko Münzenrieder et al. Oxide Thin-Film Transistors on Fibers for Smart TextilesTechnologies 2017, 5, 31; doi:10.3390/technologies5020031

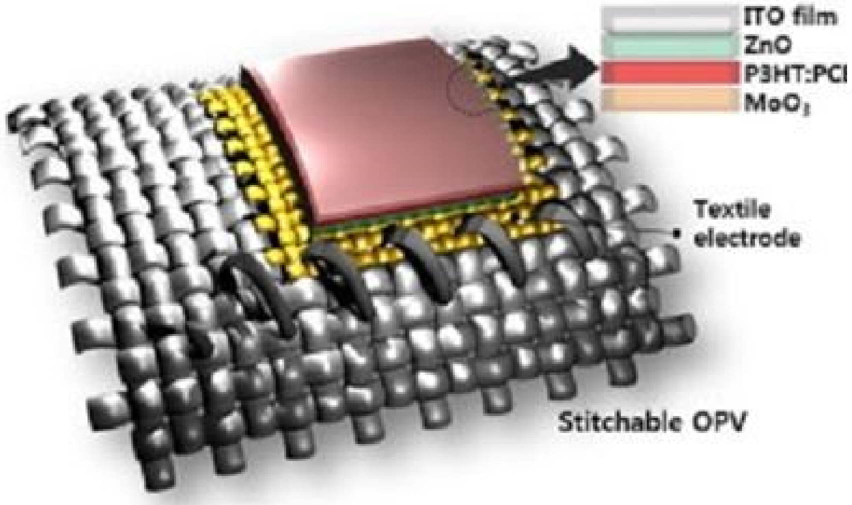

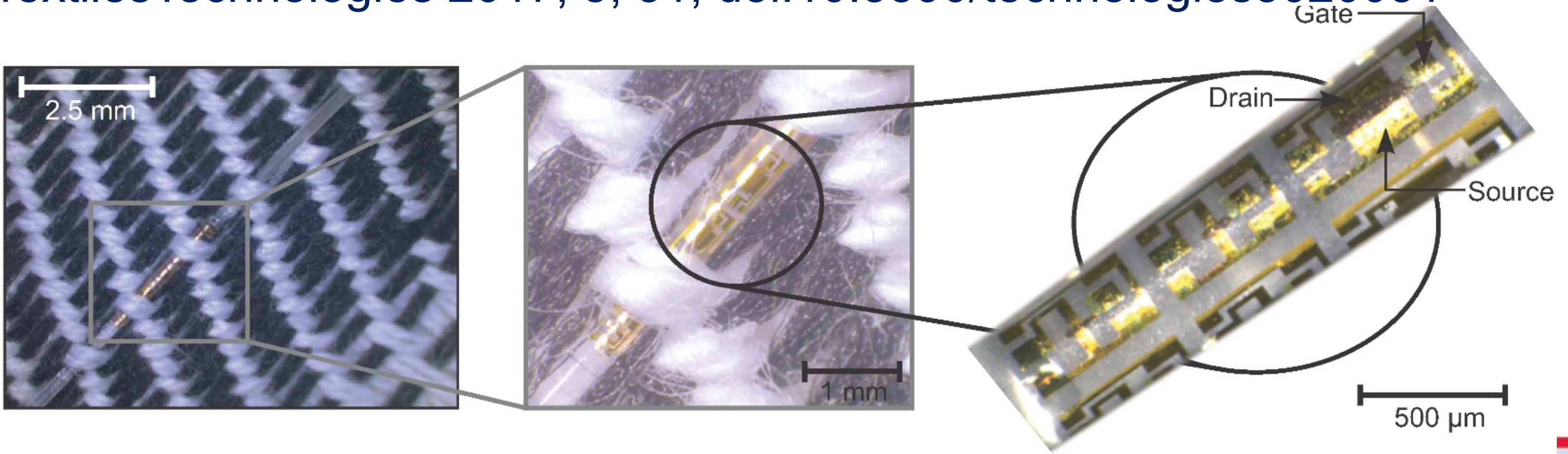

S. Lee *et al.*, ***Nano Energy* 9 (2014) 88–**

Intense pulsed light sintering of Ag NWs on fabrics for wearable heater

Pulsed light sintering to enable low-temperature and fast sintering

RUTGERS

Heating fabric using Ag NWs

Processing parameters used

- Two sets of dip coating cycles (3, called Dip-3 here and 5, called Dip-5 here) in silver NW in ethanol (2% by weight concentration)
- IPL pulse energy and on-time varied

❖ **Optimization of IPL conditions**

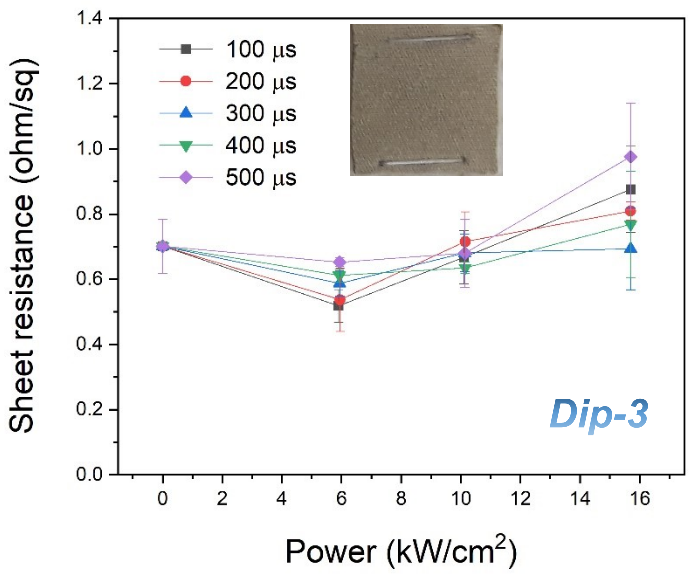

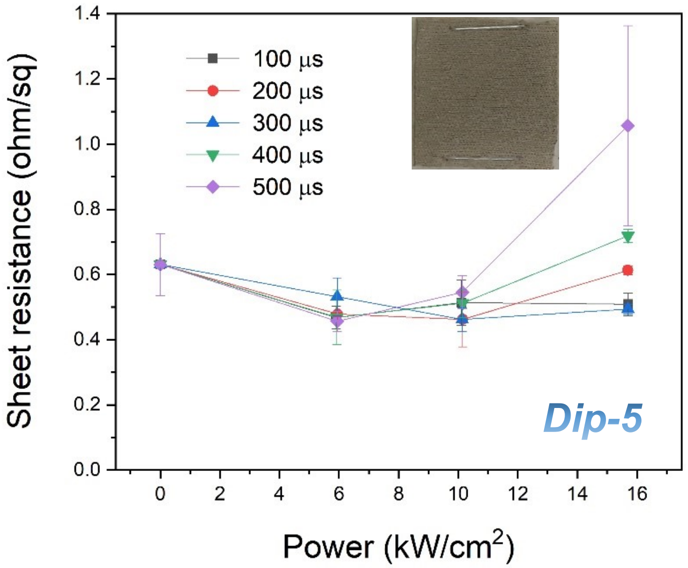

Optimal IPL conditions for dip-coating cycles

- ***Dip-3*** ➡ Single pulse, 2.0 kV, 100 μs (6 kW/cm^2)
- ***Dip-5*** ➡ Single pulse, 2.5 kV, 300 μs (10 kW/cm^2)

Heating fabric using Ag NWs

❖ SEM : Number of dip-coating cycles

	x 150	x 5K	x 20K	x 150K
Dip-1 **unsintered**	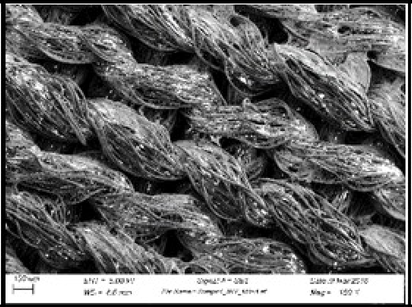	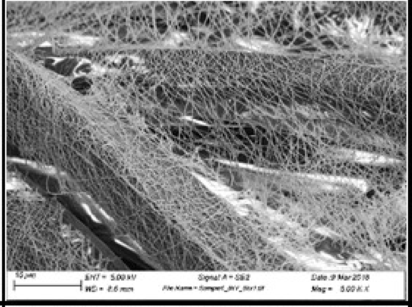	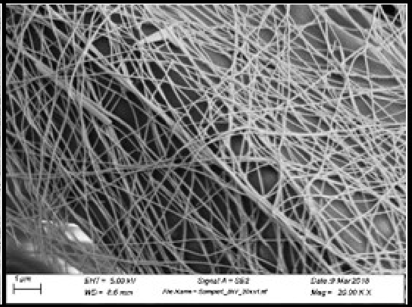	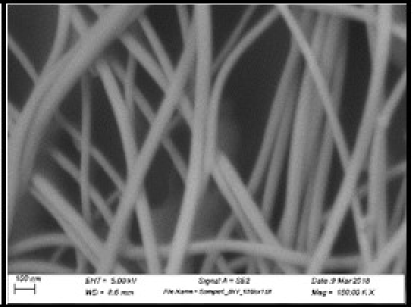
Dip-3 **unsintered**	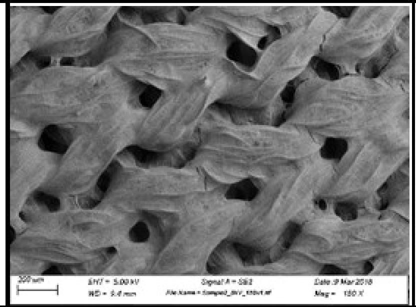	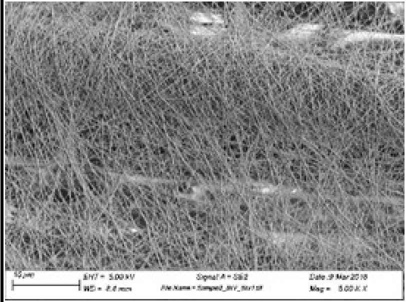	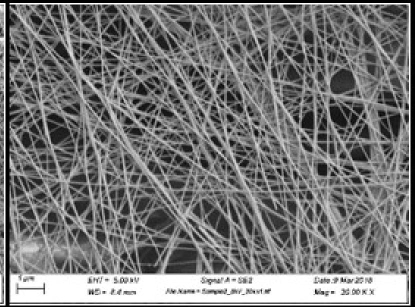	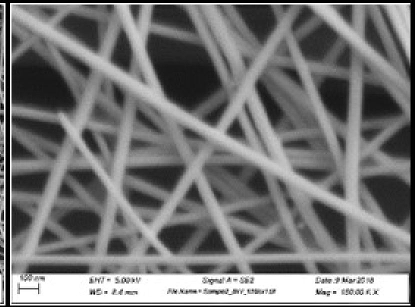
Dip-5 **unsintered**	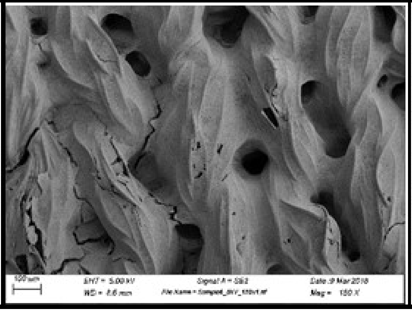	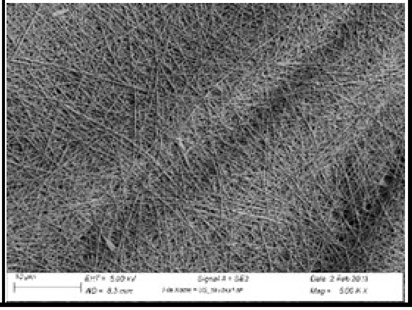	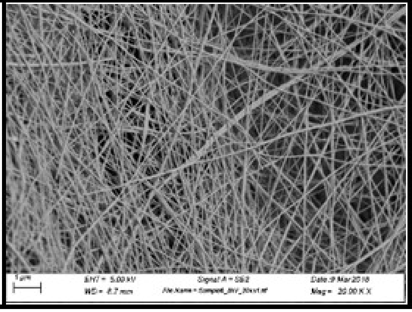	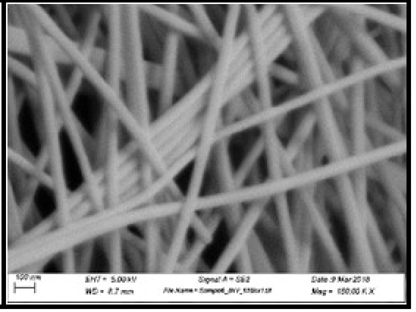

Heating fabric using Ag NWs

SEM : *Dip-3*

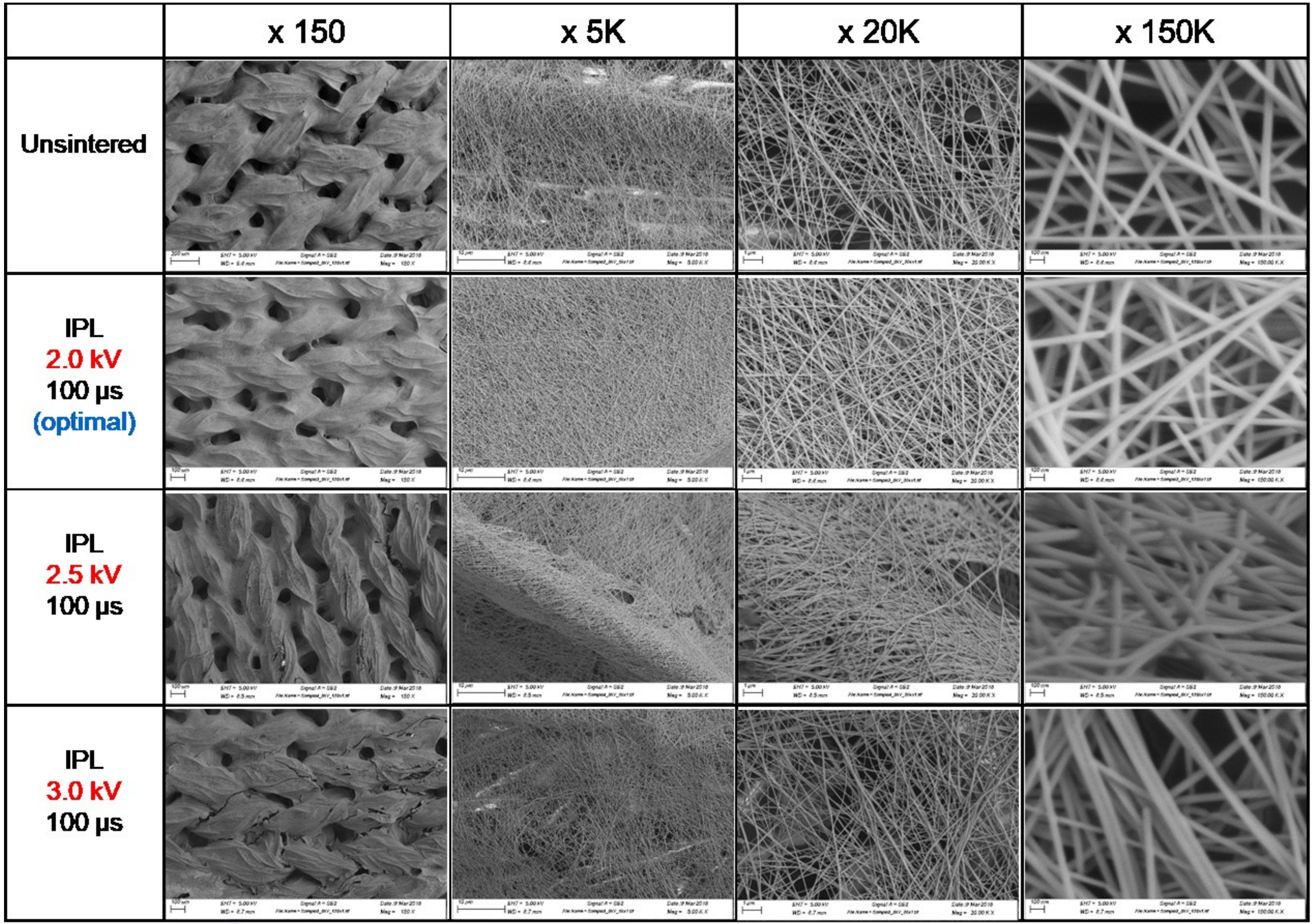

Heating fabric using Ag NWs

- **SEM : *Dip-5***

	x 150	x 5K	x 20K	x 150K
Unsintered	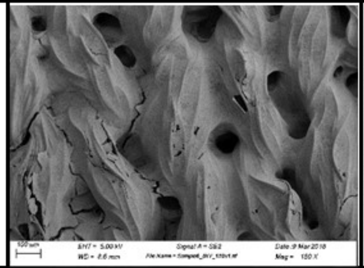	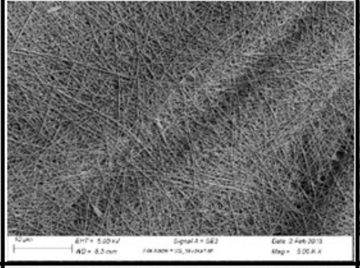	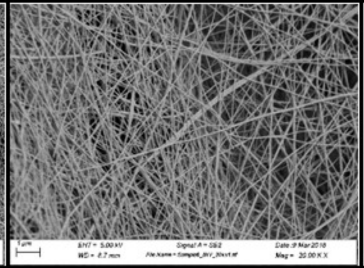	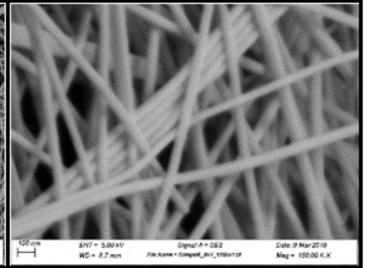
IPL 2.0 kV 300 μs	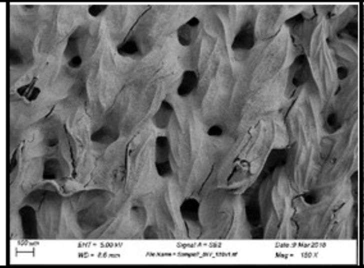	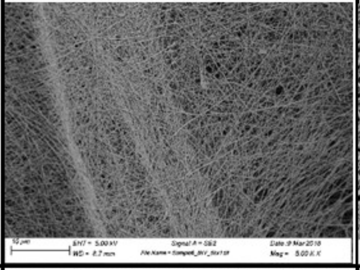	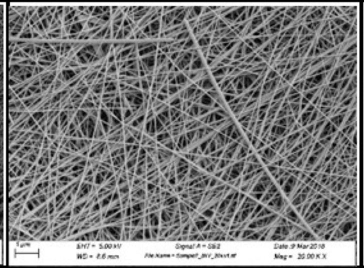	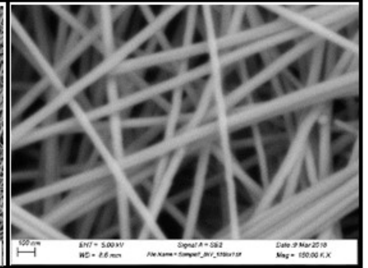
IPL 2.5 kV 300 μs (optimal)	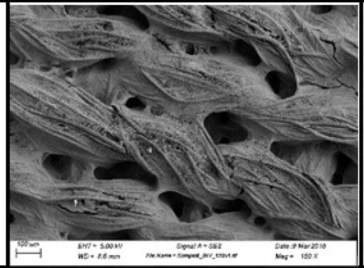	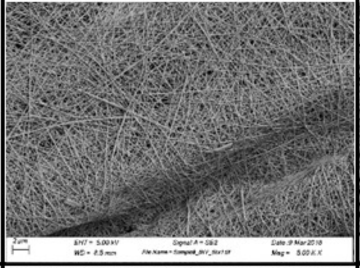	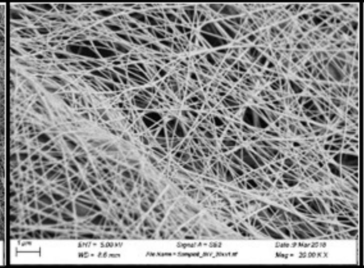	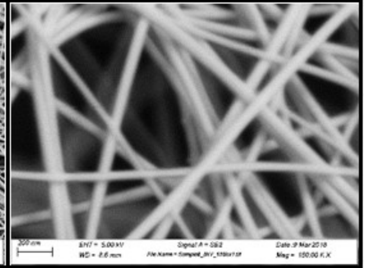
IPL 3.0 kV 300 μs	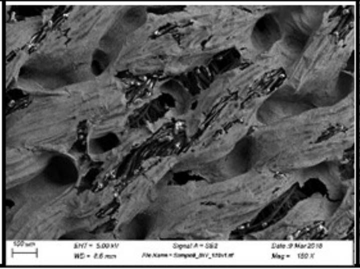	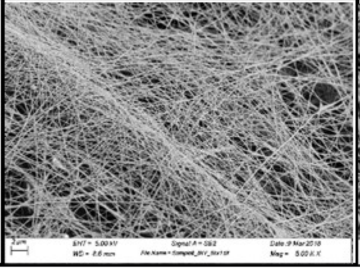	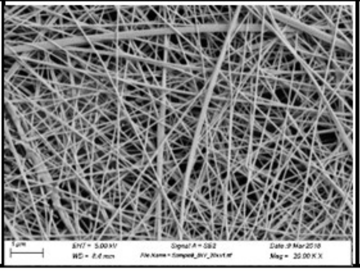	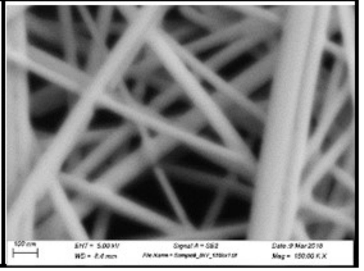

Heating fabric using Ag NWs

- ❖ **XRD**

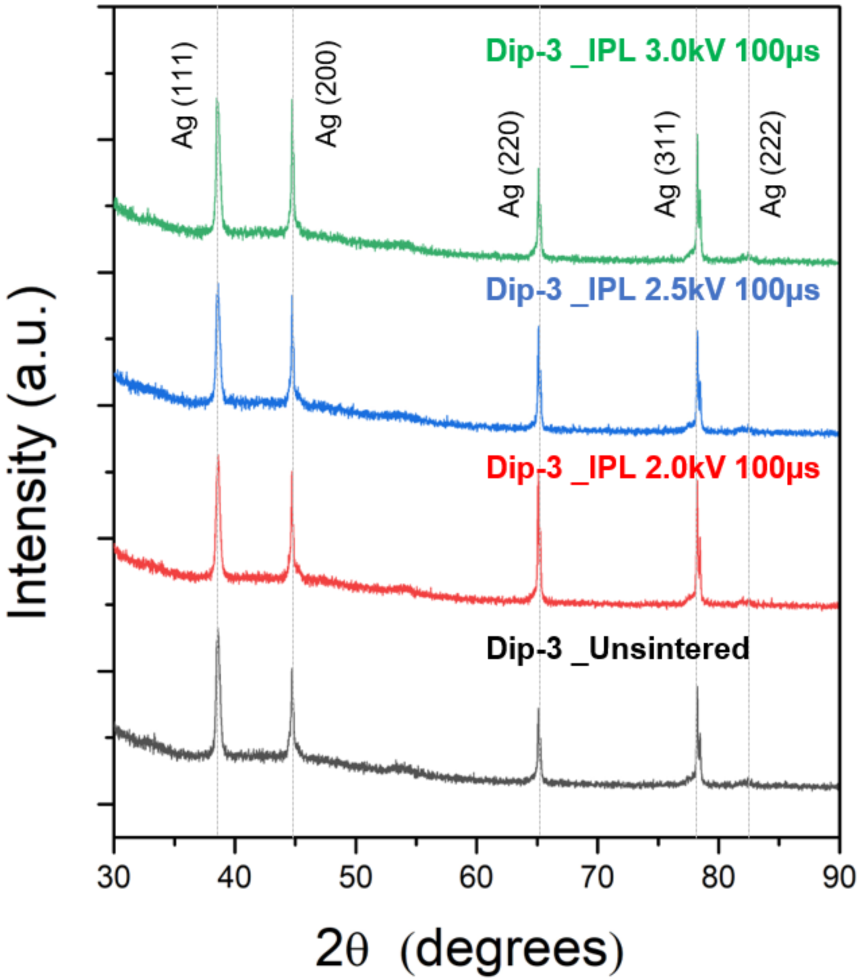

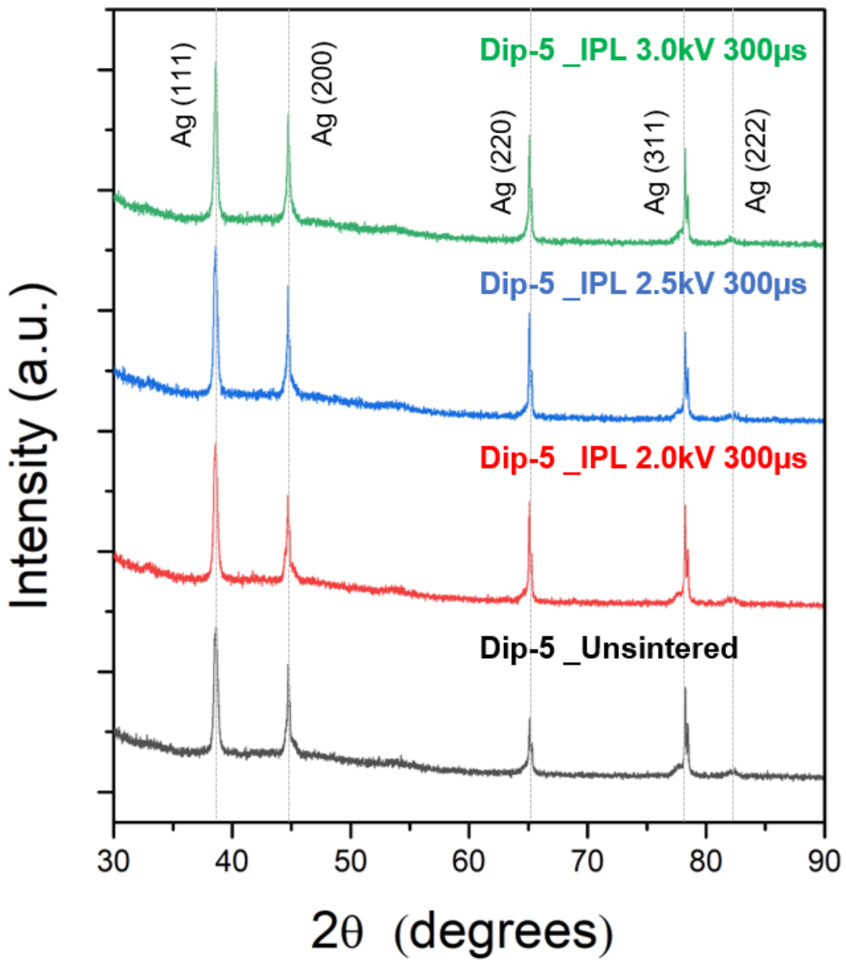

Heating fabric using Ag NWs

❖ Mechanical reliability test

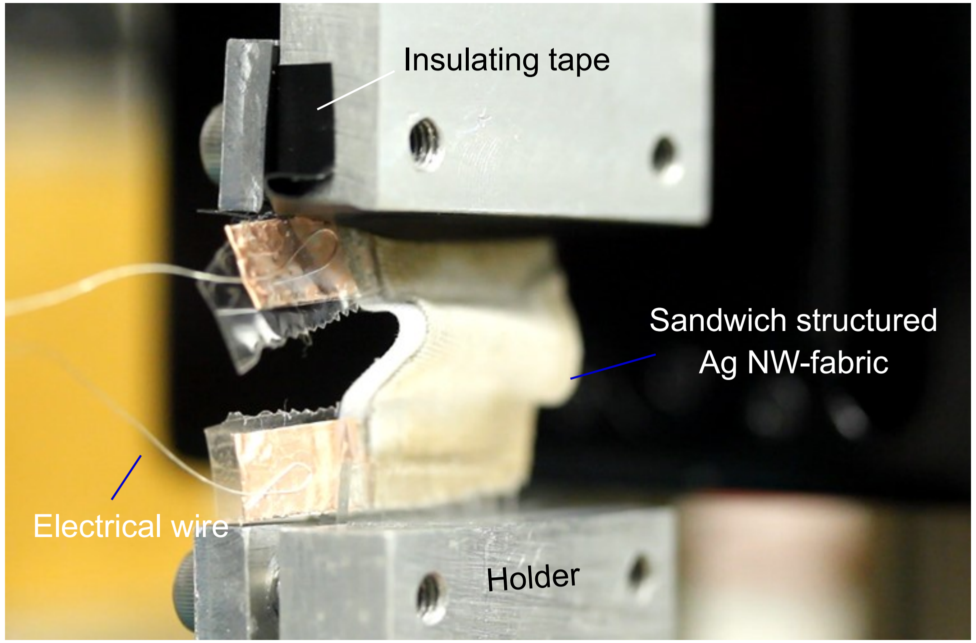

Reliability test conditions

Sample size: 30 x 20 mm
Displacement: 5 mm
Applied force: 0.15 N
Repetition cycle: 100

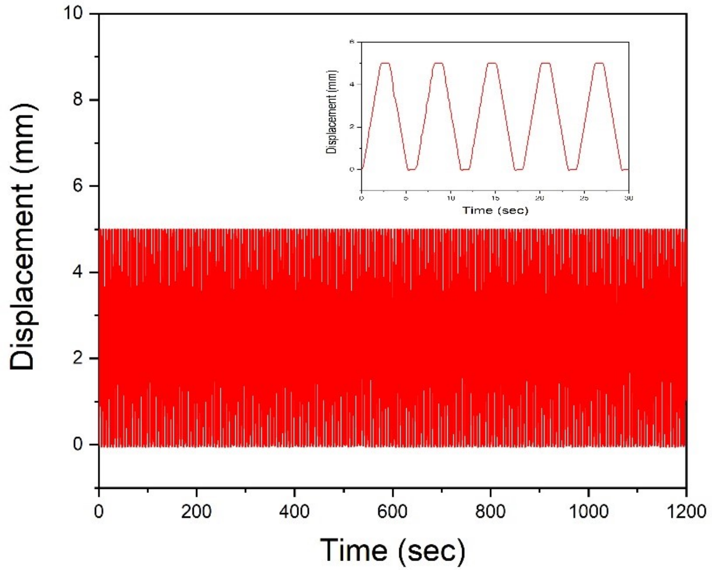

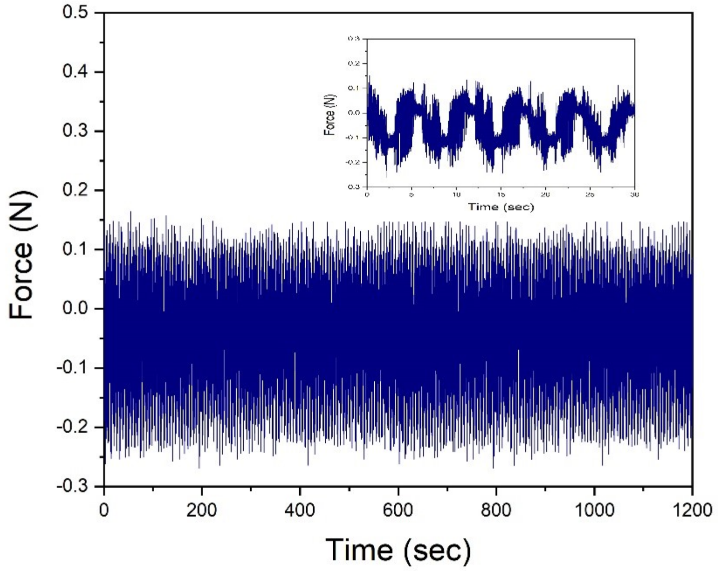

Heating fabric using Ag NWs

RUTGERS

❖ **Mechanical reliability test: Unsintered condition compared to optimal conditions shows less change in resistance upon bending**

Dip-3

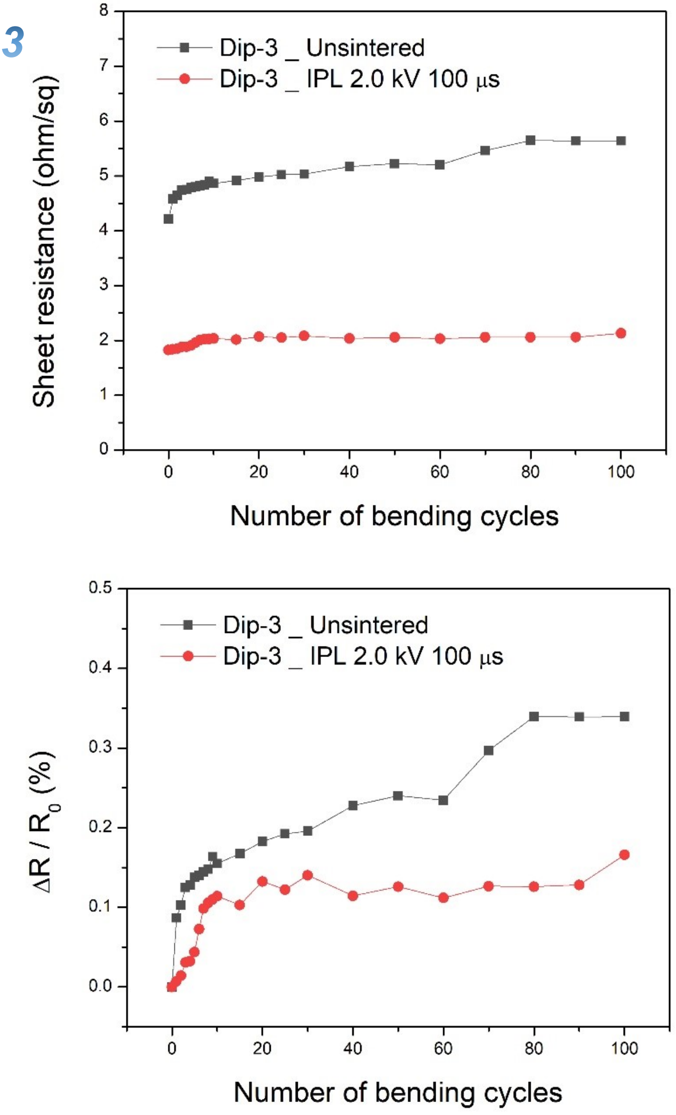

Dip-5

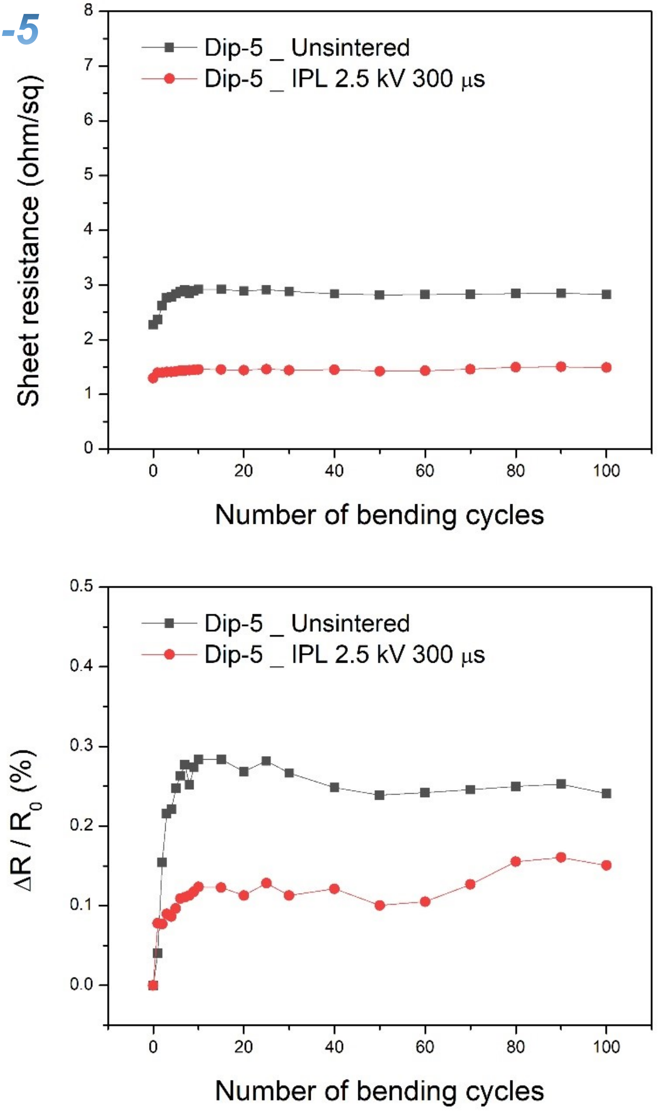

Heating fabric using Ag NWs

RUTGERS

- **Environmental test: Low temperature high humidity**

IPL sintering
Voltage: 2.0 and 2.5 kV
Pulse number: 1
Pulse duration: 100 **and** 300 μsec

Environmental test
Temperature: **25˚C**
Humidity: 75% RH
Test time: 6 hour

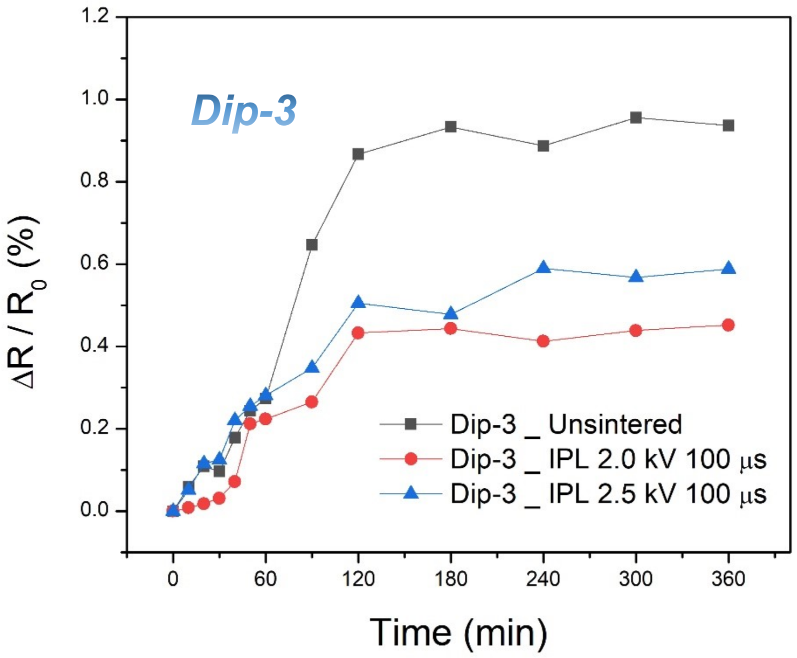

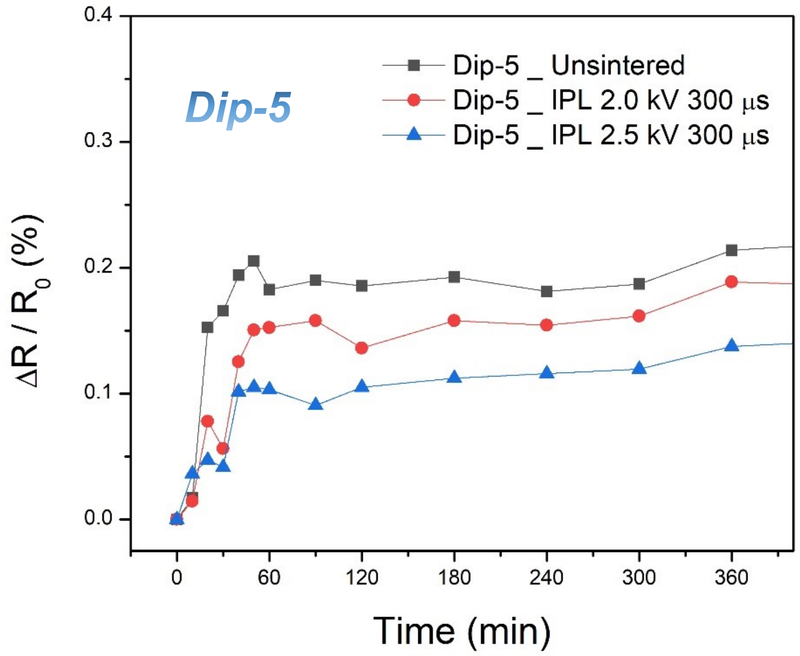

Sintered fabric is more reliable

Heating fabric using Ag NWs

❖ Environmental test: High temperature low humidity

IPL sintering
Voltage: 2.0 and 2.5 kV
Pulse number: 1
Pulse duration: 100 **and** 300 μsec

Environmental test
Temperature: **70˚C**
Humidity: 40% RH
Test time: 6 hour

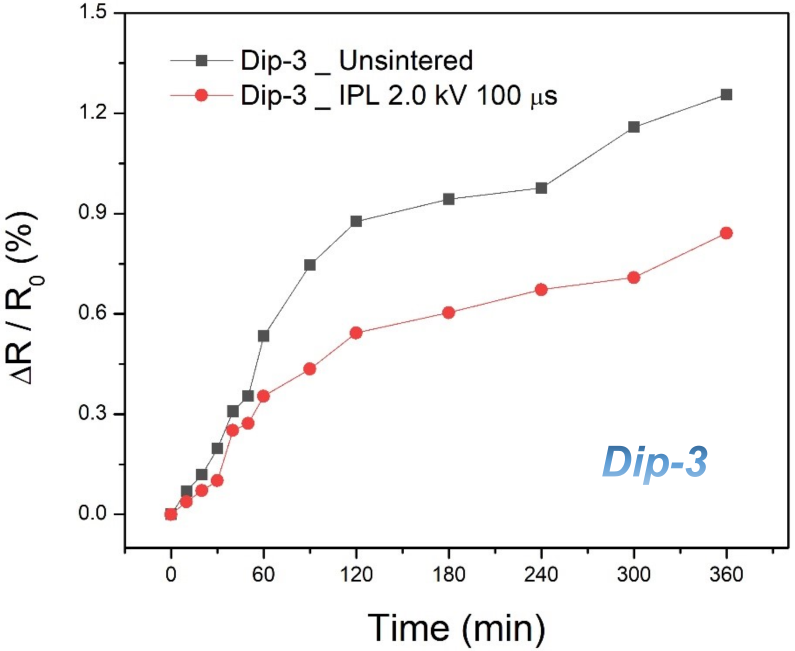

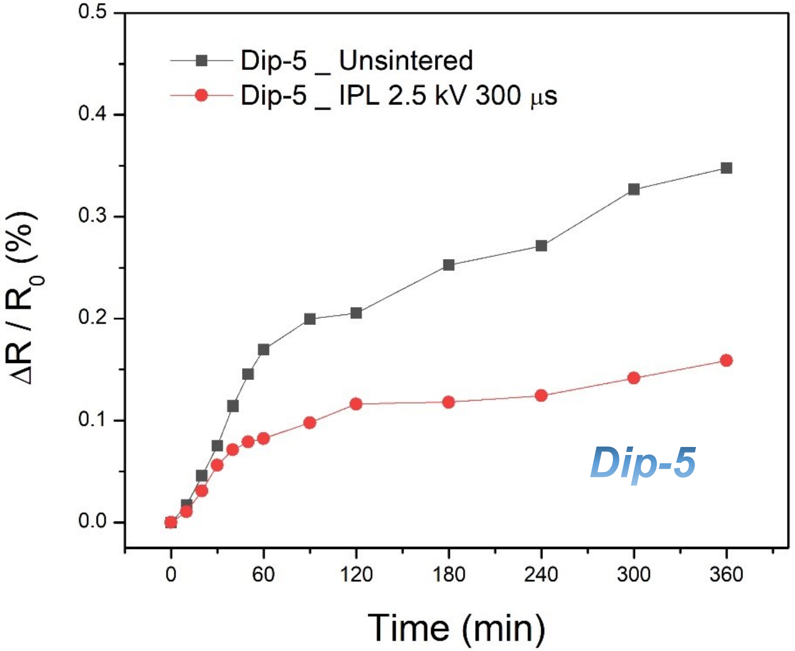

Sintered fabric is more reliable

Heating fabric using Ag NWs

RUTGERS

❖ Washing test between unsintered and optimal IPL conditions at each dip coating cycle number

IPL sintering
Voltage: 2.0 and 2.5 kV
Pulse number: 1
Pulse duration: 100 **and** 300 μsec

Washing test
Washing: DI water, 500 rpm
Washing time: 20 min
Drying condition: 80˚C, 1 hour
Number of washing cycles: 5

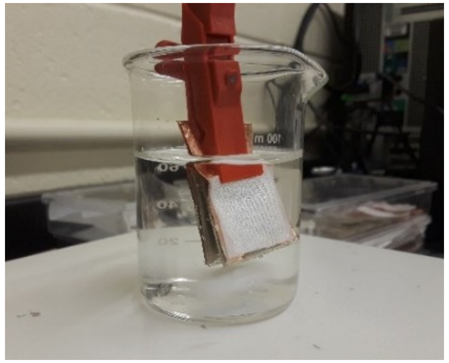

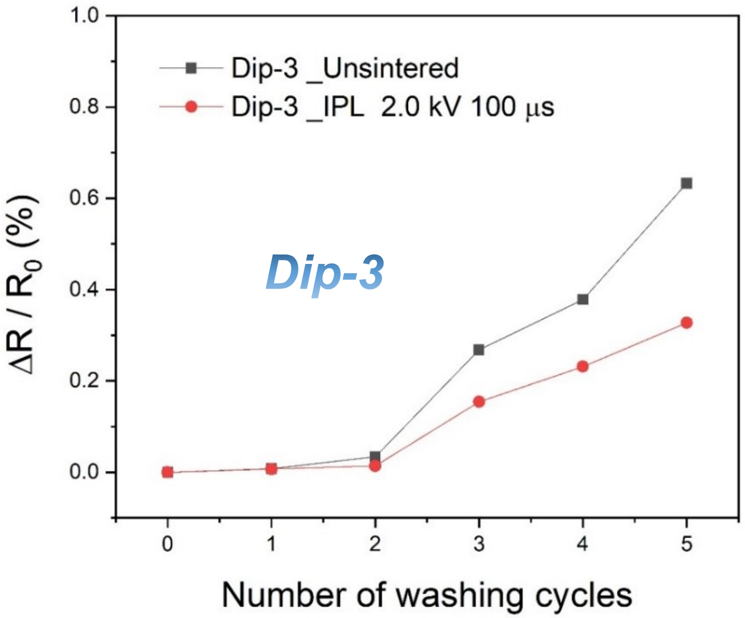

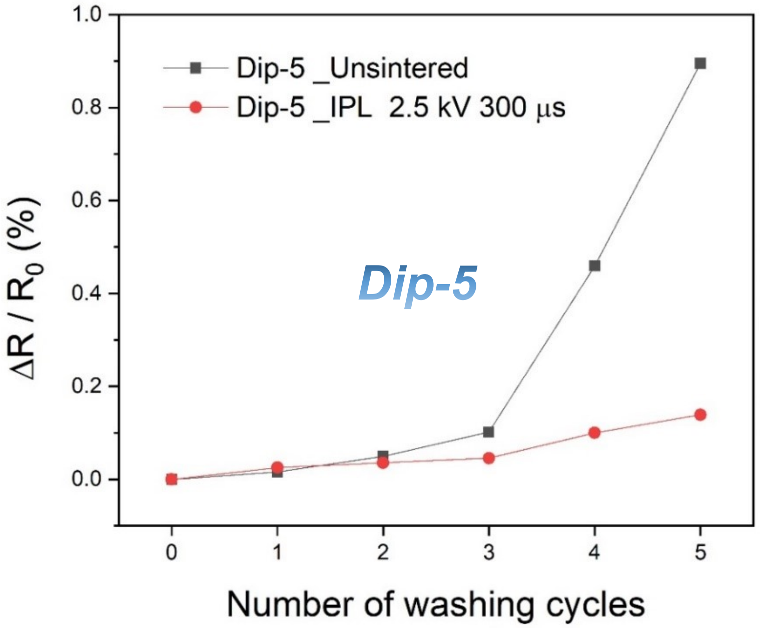

Sintered fabric is more washable, especially for the optimal condition (red) for 5 dip coating cycles

Flexible UV detector based on carbon fibers, ZnO nanorods, and Ag nanowires
Geon Jang et al. J. Mater. Chem. C, 2017, 5,4537

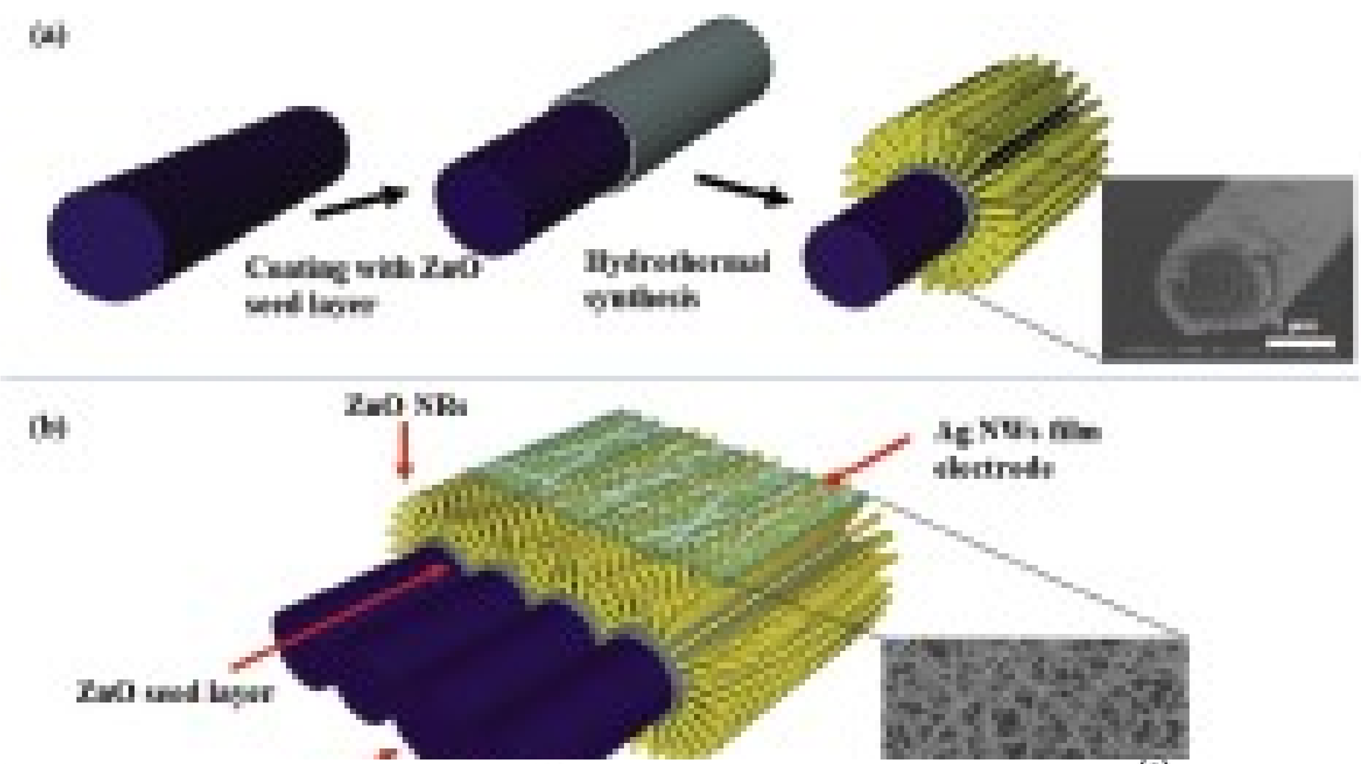

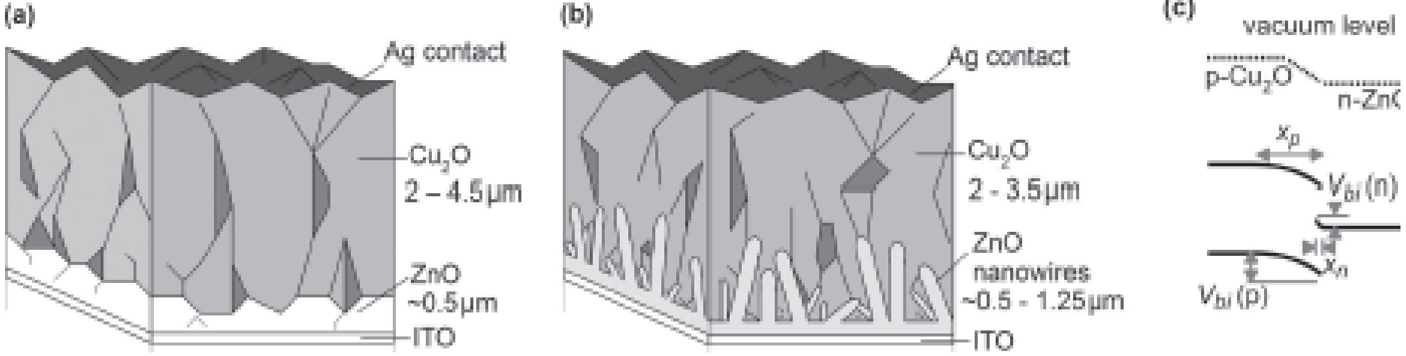

Incompatible Length Scales in Nanostructured Cu 2 O Solar Cells
Kevin P. Musselman et al. Adv. Funct. Mater. 2012, 22, 2202.

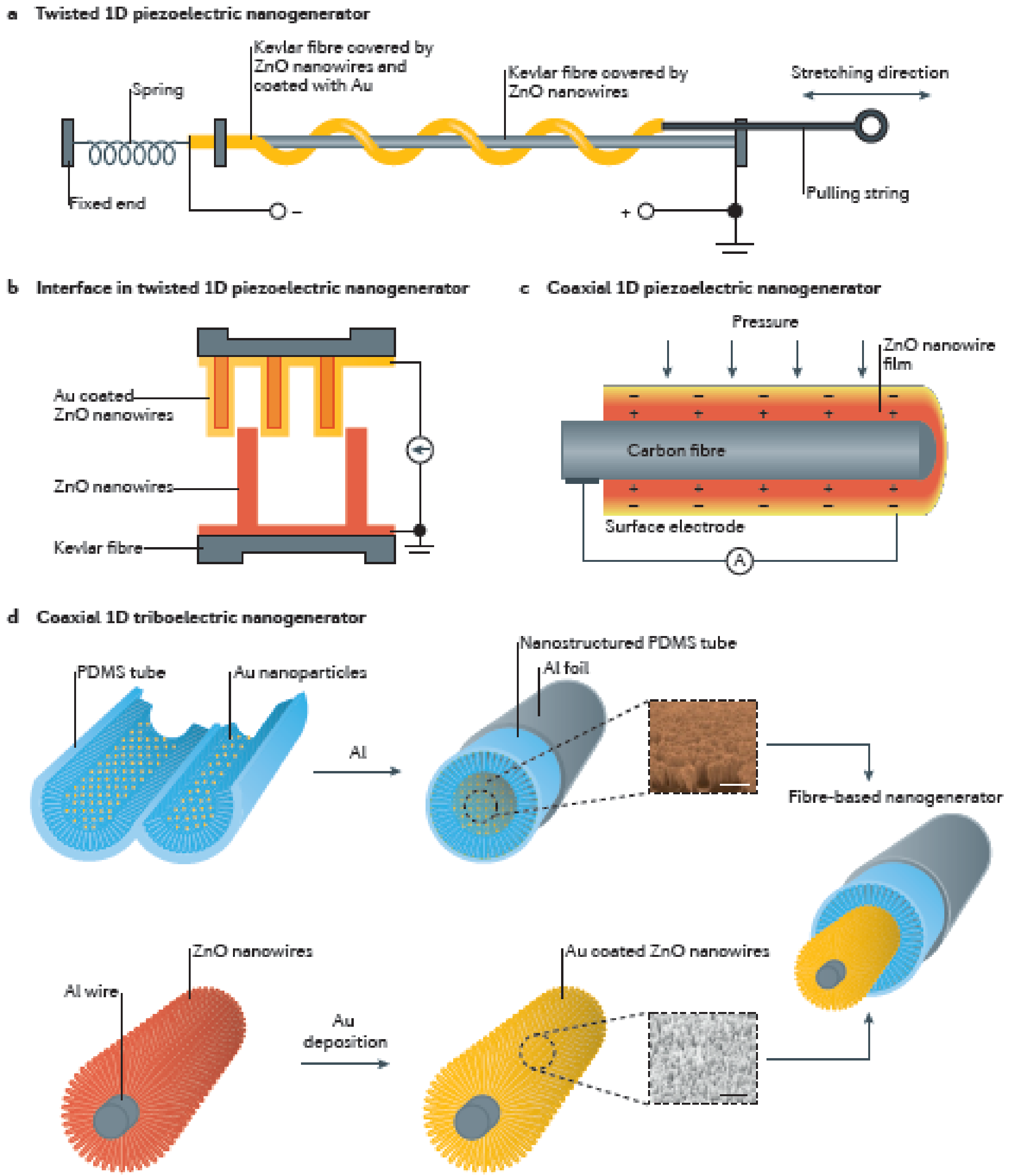

Pan, C. et al. Fiber-based hybrid nanogenerators for/as self-powered systems in biological liquid. Angew. Chem. Int. Ed. 50, 11192–11196 (2011).

Microreactor-Assisted Nanomaterial Deposition

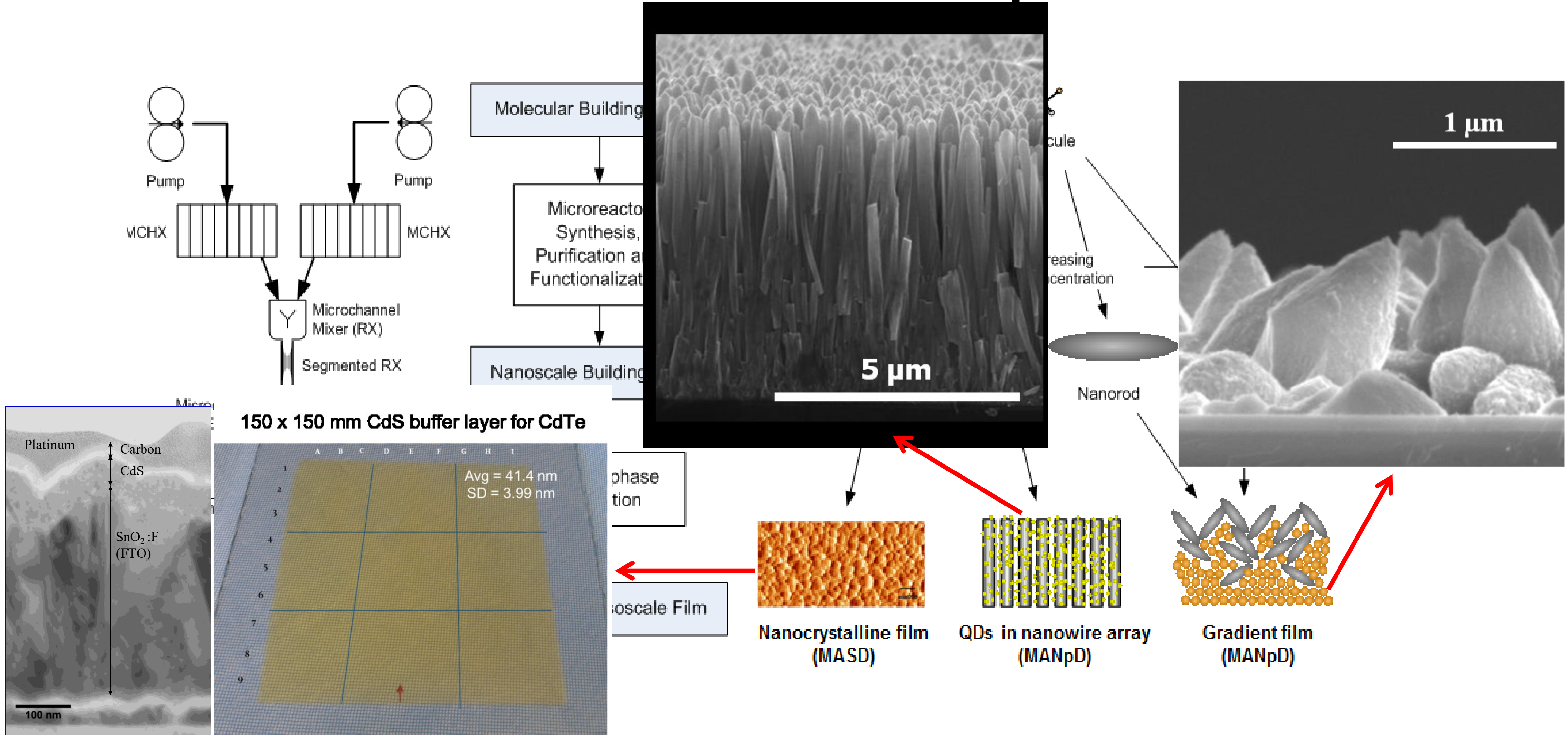

CBD-Chemical Bath Deposition?

Features:
- **Low temperature**
- **Low cost**
- **Large area**
- **Conformal**

Photodetector

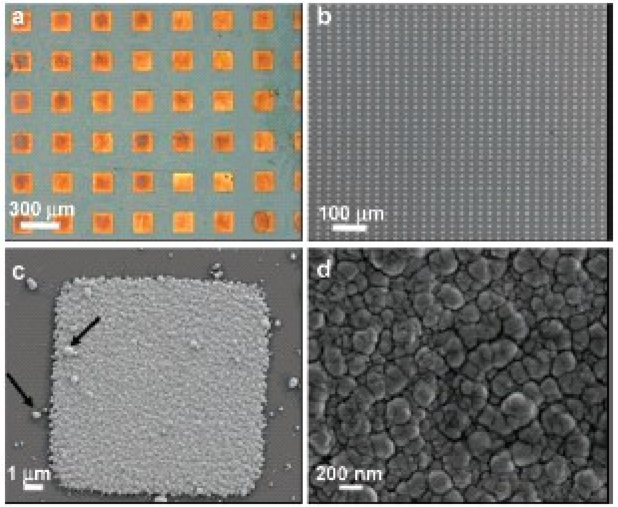

Photodetector Arrays Directly Assembled onto Polymer Substrates from Aqueous Solution

Fairland F. Amos, Stephen A. Morin, Jeremy A. Streifer, Robert J. Hamers, and Song Jin*

J. AM. CHEM. SOC. ■ VOL. 129, NO. 46, 2007

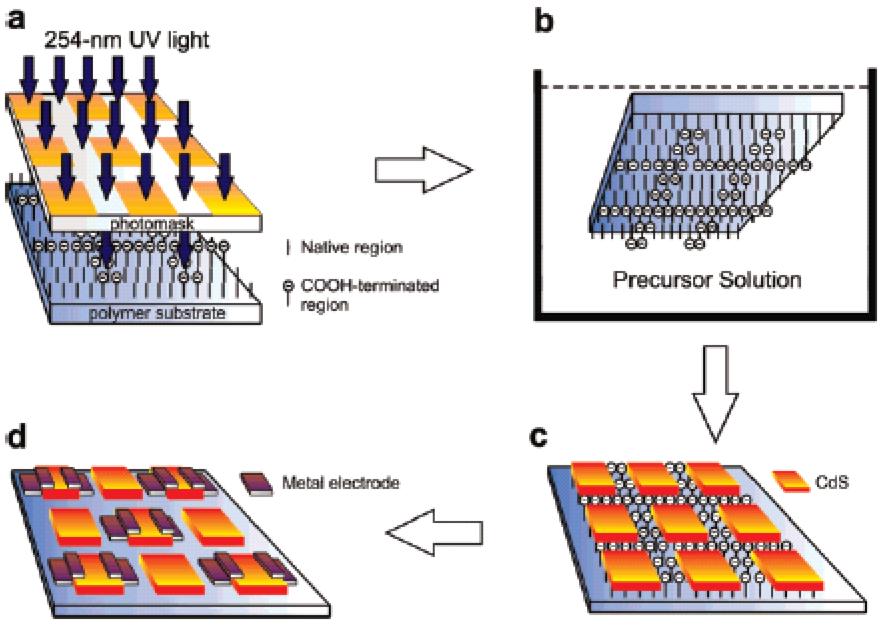

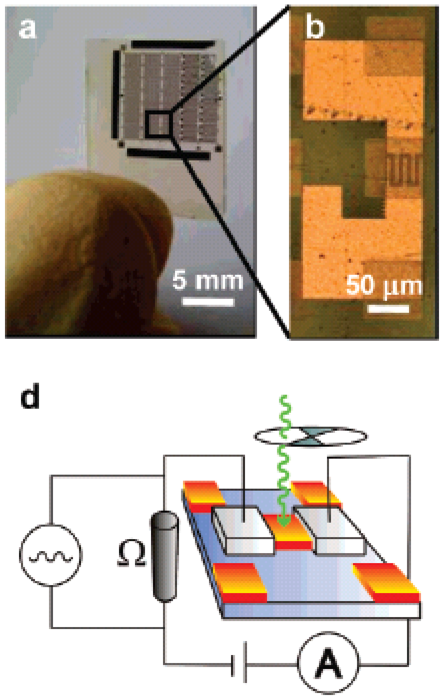

NANO LETTERS
pubs.acs.org/NanoLett

High-Performance Nanostructured Inorganic−Organic Heterojunction Solar Cells

Jeong Ah Chang,[†,§] Jae Hui Rhee,[†,§] Sang Hyuk Im,[†] Yong Hui Lee,[†] Hi-jung Kim,[†] Sang Il Seok,[*,†] Md. K. Nazeeruddin,[‡] and Michael Gratzel[‡]

[†]KRICT-EPFL Global Research Laboratory, Advanced Materials Division, Korea Research Institute of Chemical Technology, 19 Sinseongno, Yuseong, Daejeon 305-600, Republic of Korea, and [‡]Laboratory for Photonics and Interfaces, Institute of Chemical Sciences and Engineering, School of Basic Science, Swiss Federal Institute of Technology, CH-1015 Lausanne, Switzerland

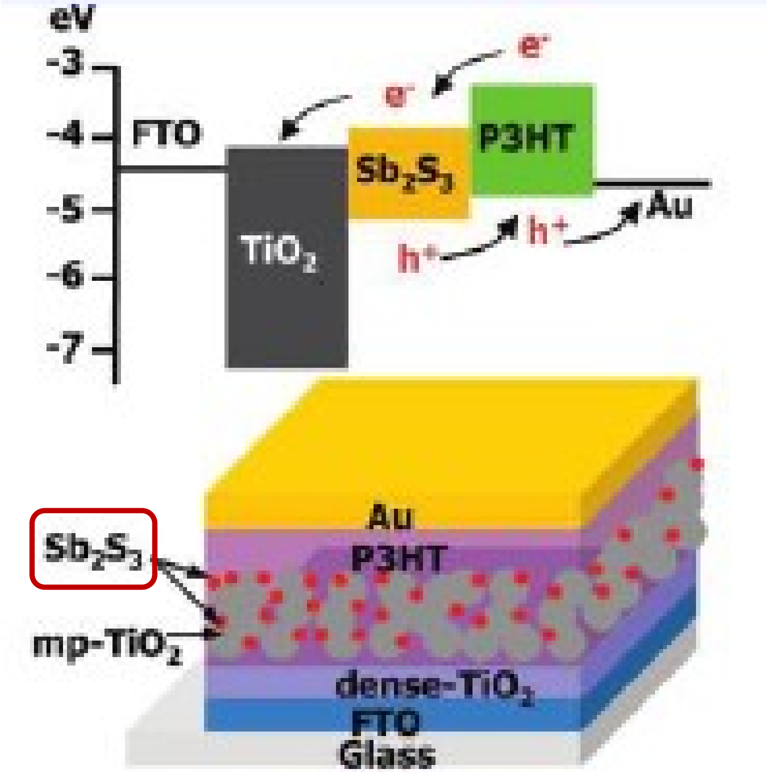

TABLE 1. Summary of Device Parameters (Short-Circuit Current Density, J_{sc}; Open-Circuit Voltage, V_{oc}; Fill Factor, FF; and Overall Conversion Efficiencies) Obtained from mp-TiO$_2$/P3HT and mp-TiO$_2$/Sb$_2$S$_3$/P3HT Shown in Figure 1d[a]

CBD time (h) for Sb$_2$S$_3$	J_{sc} [mA cm^{-2}]	V_{oc} [mV]	FF [%]	Eff [%]
mp-TiO$_2$/P3HT/Au	0.63	475	29.2	0.092
1	5.3	424	64.1	1.48
2	9.1	465	65.5	2.92
3	12.3	556	69.9	5.06
4	11.0	535	63.8	3.97

[a] Masks (0.085 cm^2) made of black plastic tape were attached to each cell before measurement under illumination (94.5 mW cm^{-2}).

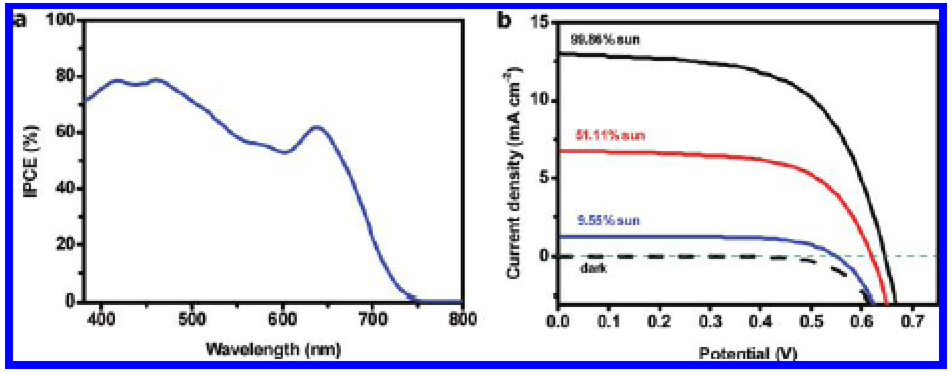

A Typical CBD CdS Growth Curve with Four CBD Deposition Regimes

Schematic Diagram of CBD CdS Growth Mechanism

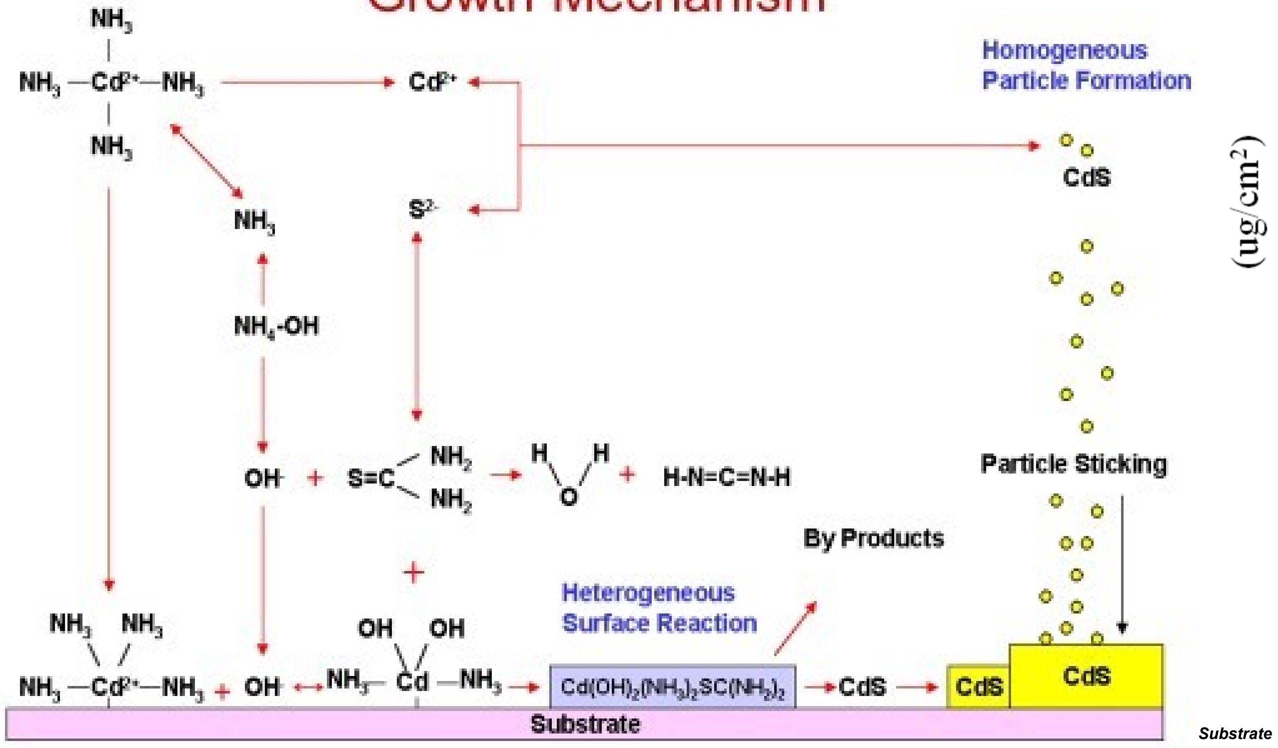

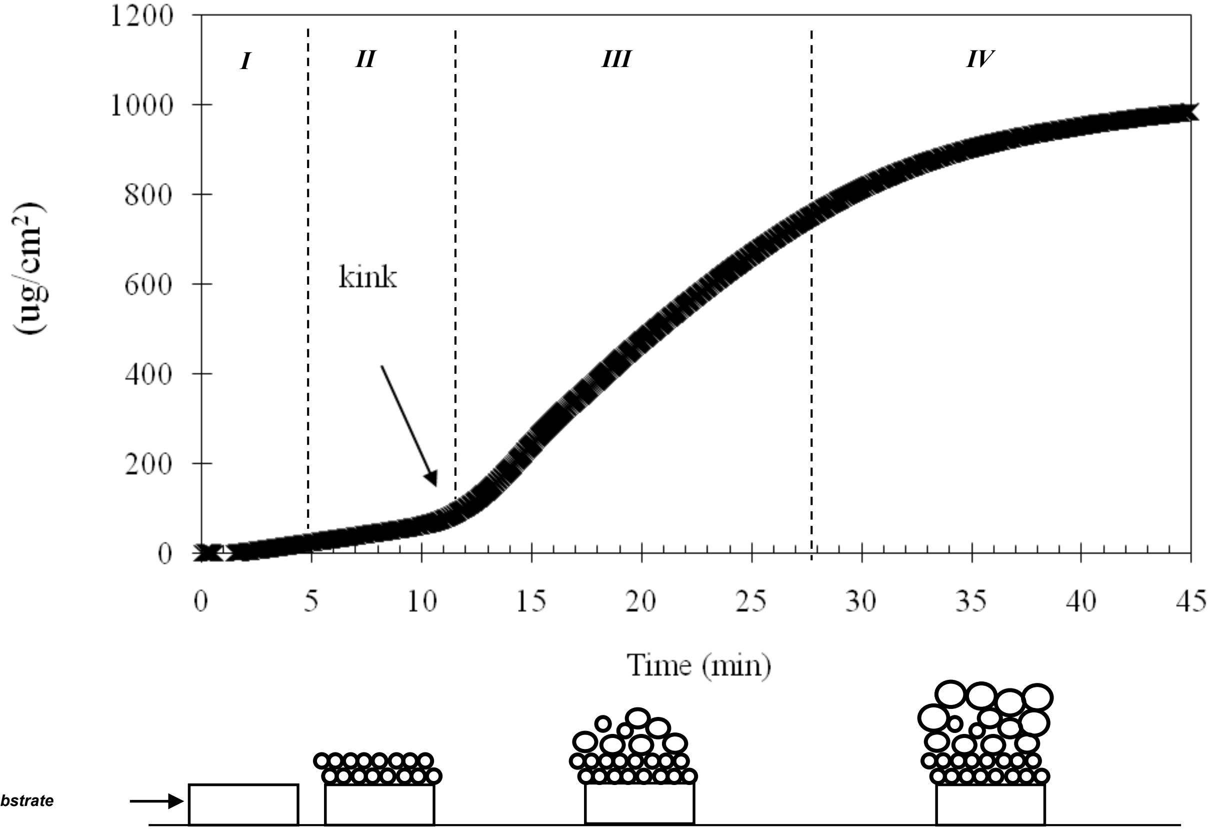

P.-H. Mugdur, Y.-J. Chang, S.-Y. Han, A.A. Morrone, S.-O. Ryu, T.J. Lee, C.-H. Chang, “A Comparison of Chemical Bath Deposition of CdS from a Batch Reactor and a Continuous Flow Microreactor,” *J. Electrochem. Soc.* 154(9), D482-D488, 2007.

I : Induction Regime, II : Compact layer growth regime, III : Porous layer regime, IV : Saturation regimes

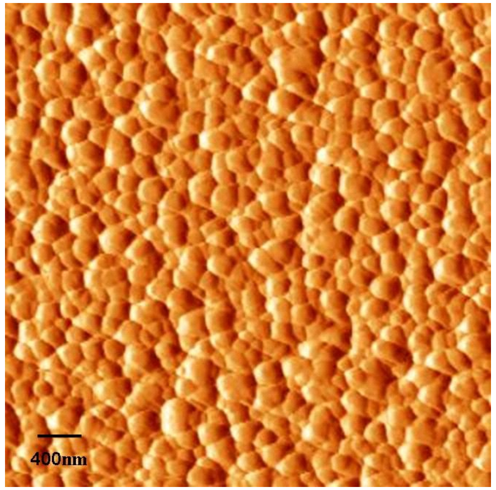

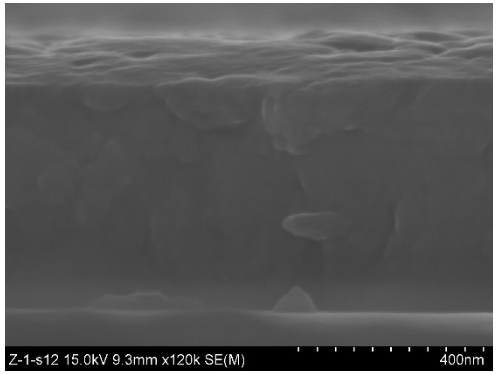

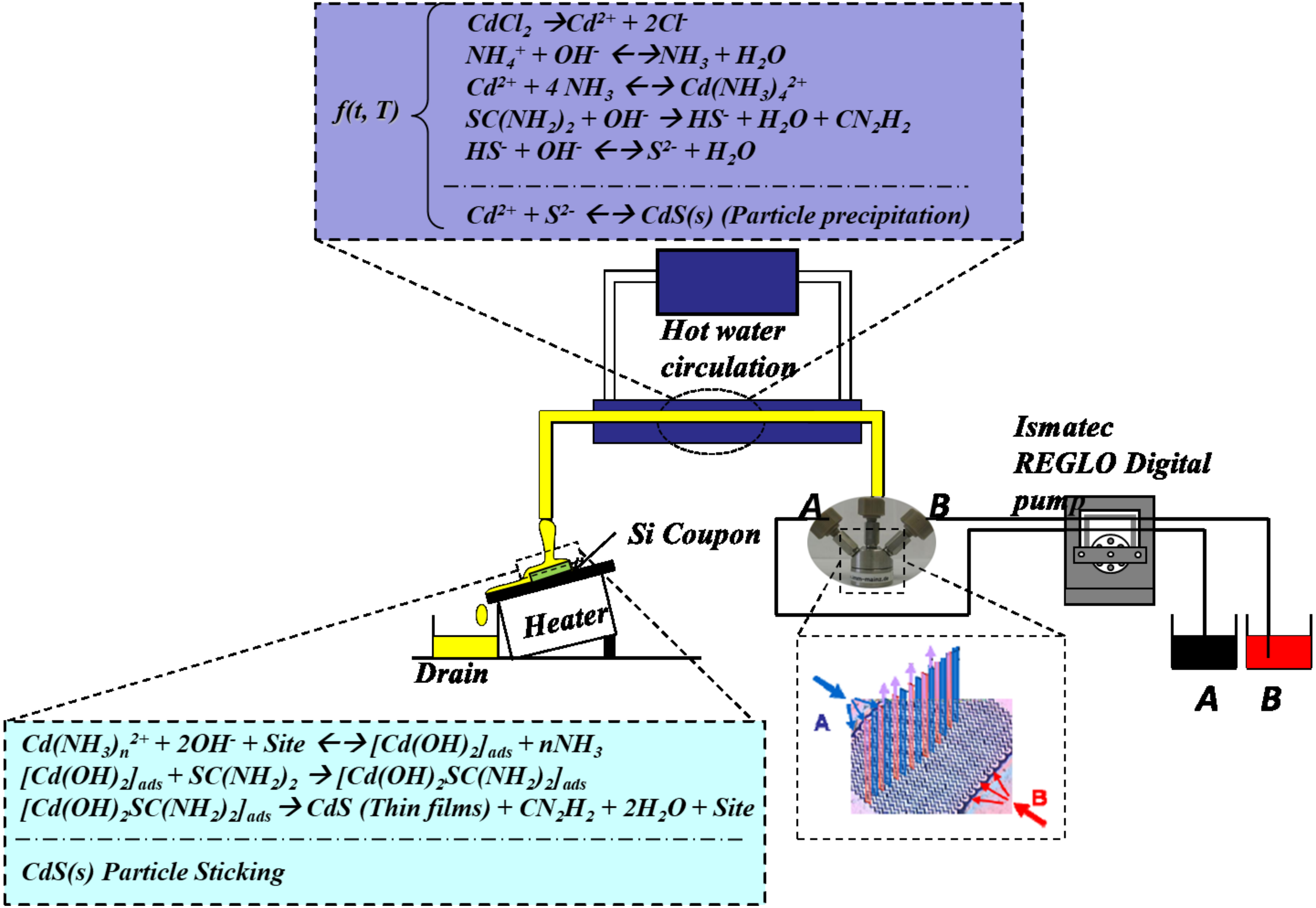

$$f(t, T)\left\{\begin{array}{l} CdCl_2 \rightarrow Cd^{2+} + 2Cl^- \\ NH_4^+ + OH^- \leftrightarrow NH_3 + H_2O \\ Cd^{2+} + 4\,NH_3 \leftrightarrow Cd(NH_3)_4^{2+} \\ SC(NH_2)_2 + OH^- \rightarrow HS^- + H_2O + CN_2H_2 \\ HS^- + OH^- \leftrightarrow S^{2-} + H_2O \\ \hline Cd^{2+} + S^{2-} \leftrightarrow CdS(s)\ \text{(Particle precipitation)} \end{array}\right.$$

$$Cd(NH_3)_n^{2+} + 2OH^- + Site \leftrightarrow [Cd(OH)_2]_{ads} + nNH_3$$

$$[Cd(OH)_2]_{ads} + SC(NH_2)_2 \rightarrow [Cd(OH)_2SC(NH_2)_2]_{ads}$$

$$[Cd(OH)_2SC(NH_2)_2]_{ads} \rightarrow CdS\ \text{(Thin films)} + CN_2H_2 + 2H_2O + Site$$

CdS(s) Particle Sticking

Chemical Nanoparticle Deposition

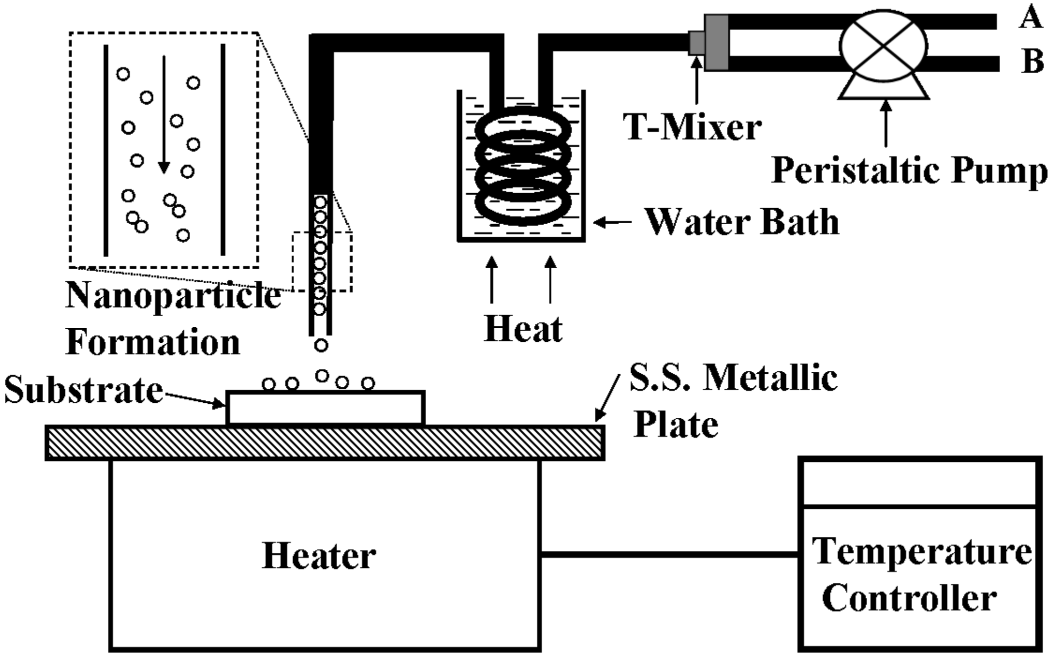

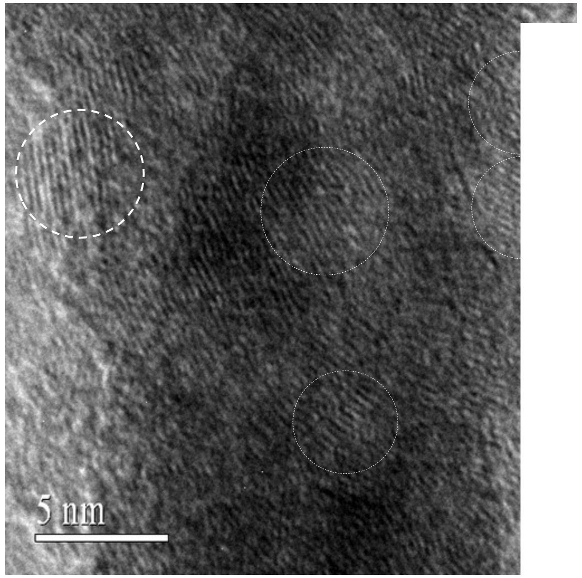

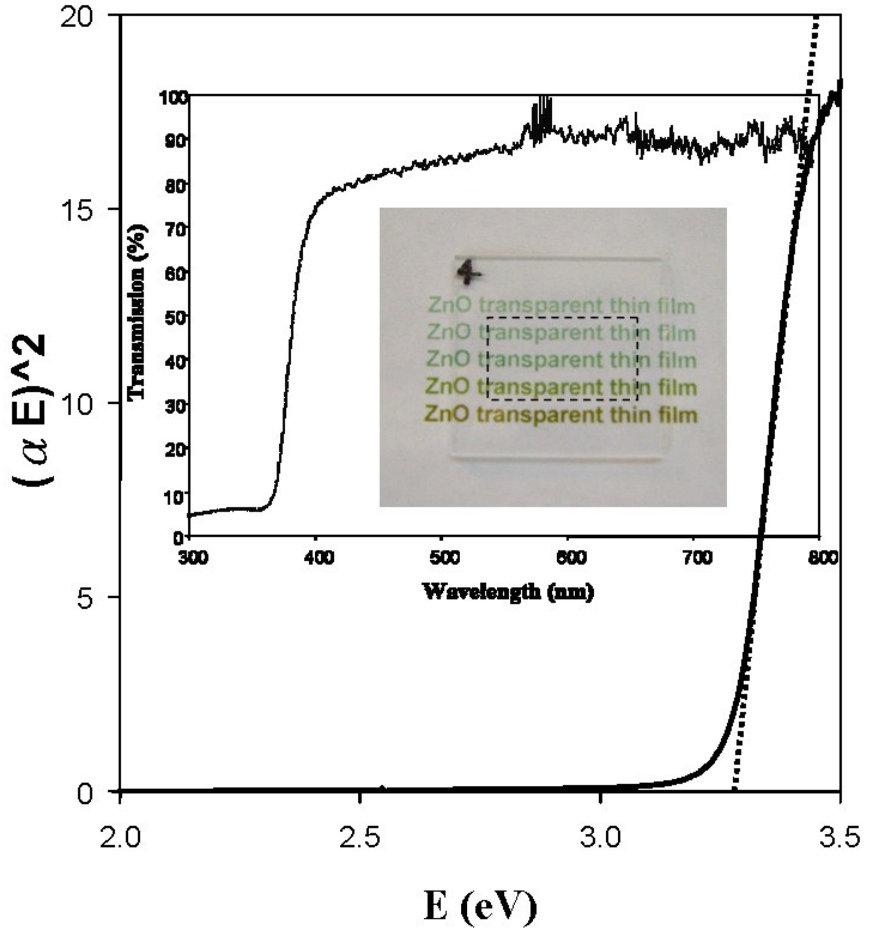

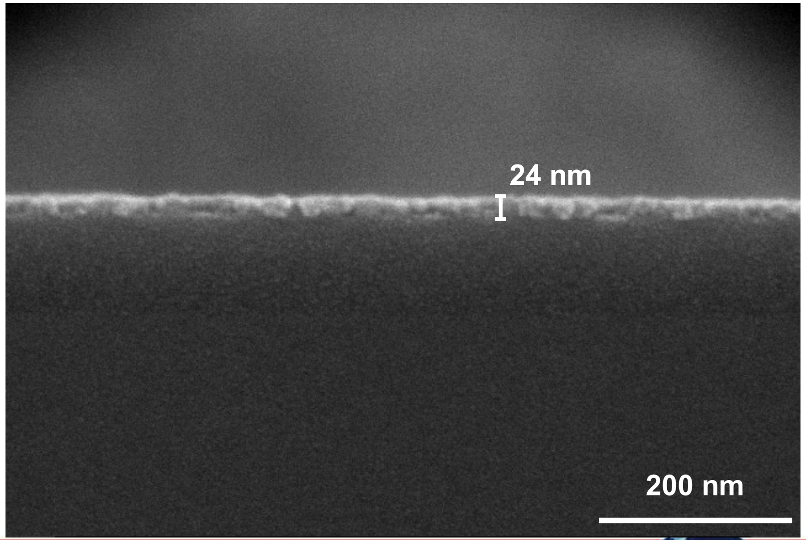

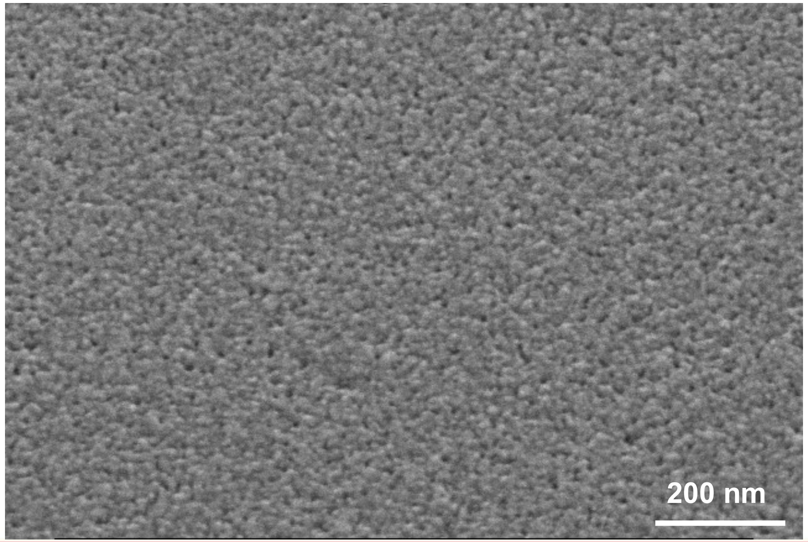

S.-Y. Han, Y-J. Chang, D.-H. Lee, S.-O. Ryu, T.J. Lee, and C-H. Chang, "Chemical Nanoparticle Deposition of Transparent ZnO Thin Films," Electrochemical and Solid-State Letters, 10(1) K1-K5, 2007.

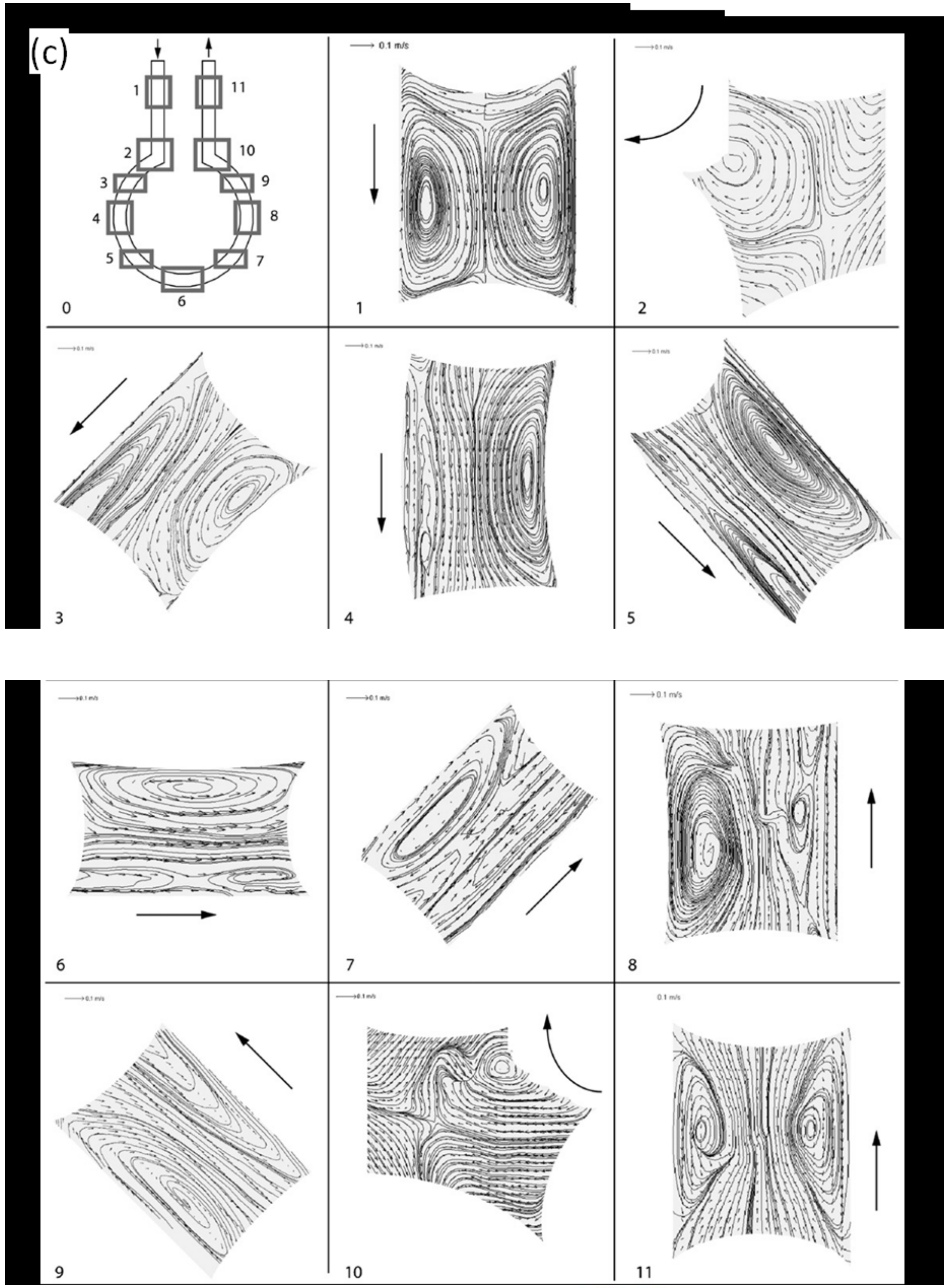

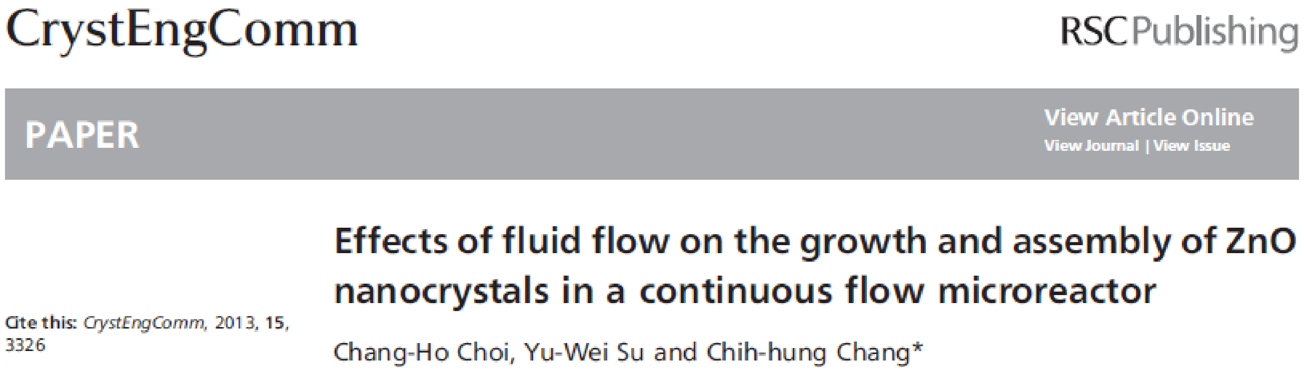
CrystEngComm

RSCPublishing

PAPER

View Article Online
View Journal | View Issue

Cite this: *CrystEngComm*, 2013, 15, 3326

Effects of fluid flow on the growth and assembly of ZnO nanocrystals in a continuous flow microreactor

Chang-Ho Choi, Yu-Wei Su and Chih-hung Chang*

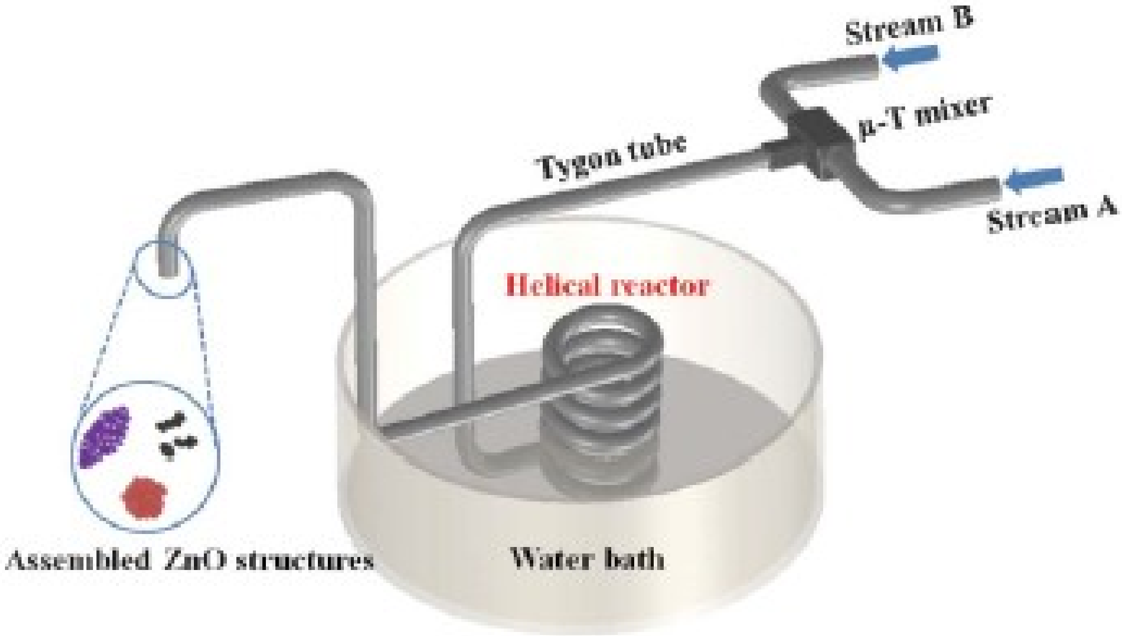

Generation of Dean vortices in helical reactor

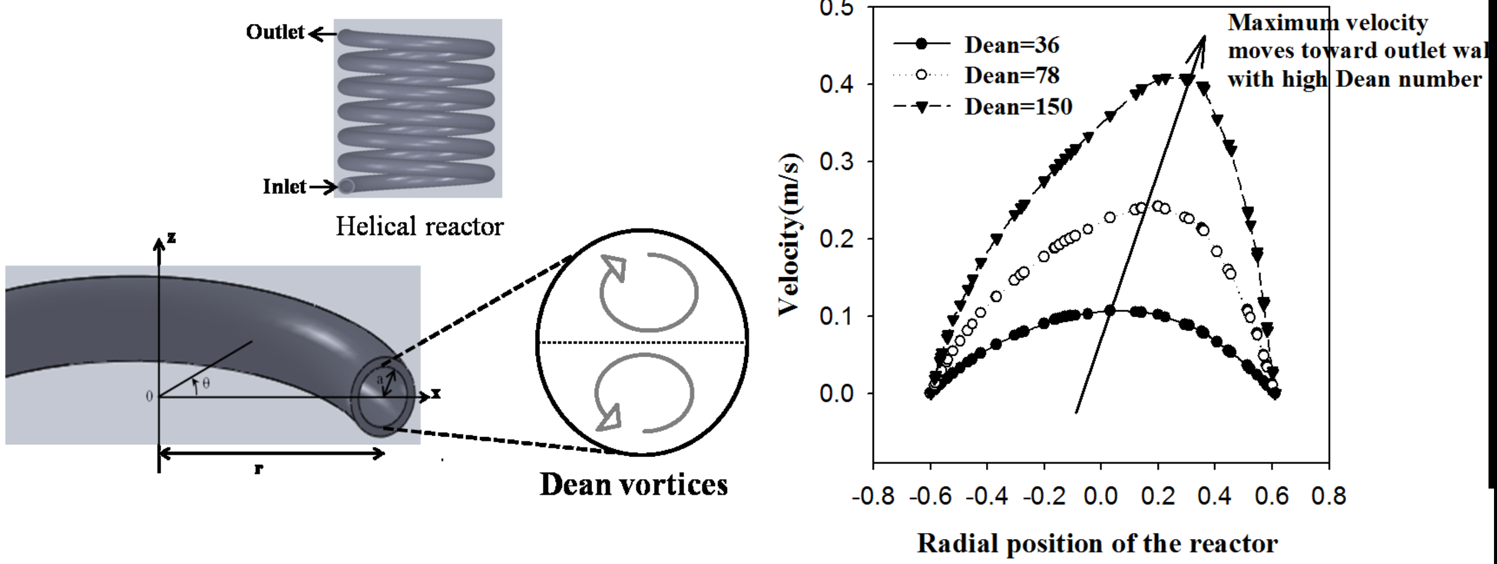

Dean vortices creation in helical reactor

$$K = \mathrm{Re}\sqrt{\frac{d}{R}}$$

- K Dean number
- Re: Reynolds number
- d: Hydraulic diameter
- R: Mean radius of curvature of channel

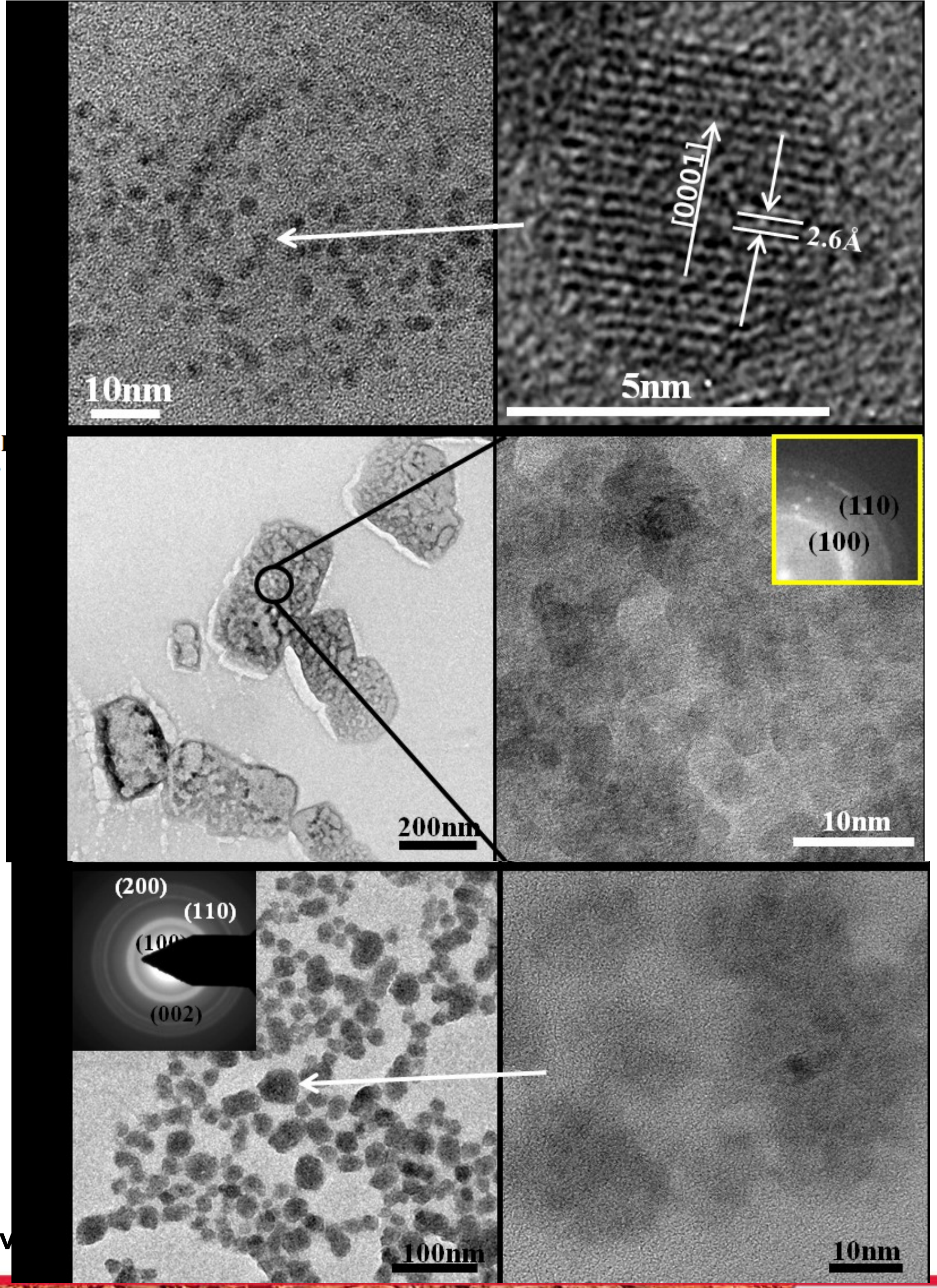

a, individual nanocrystals at 6.8 mL min^{-1}.
b, rectangular assembly at 14.7 mL min^{-1}.
c, spherical assembly at 28.1 mL min^{-1} respectiv

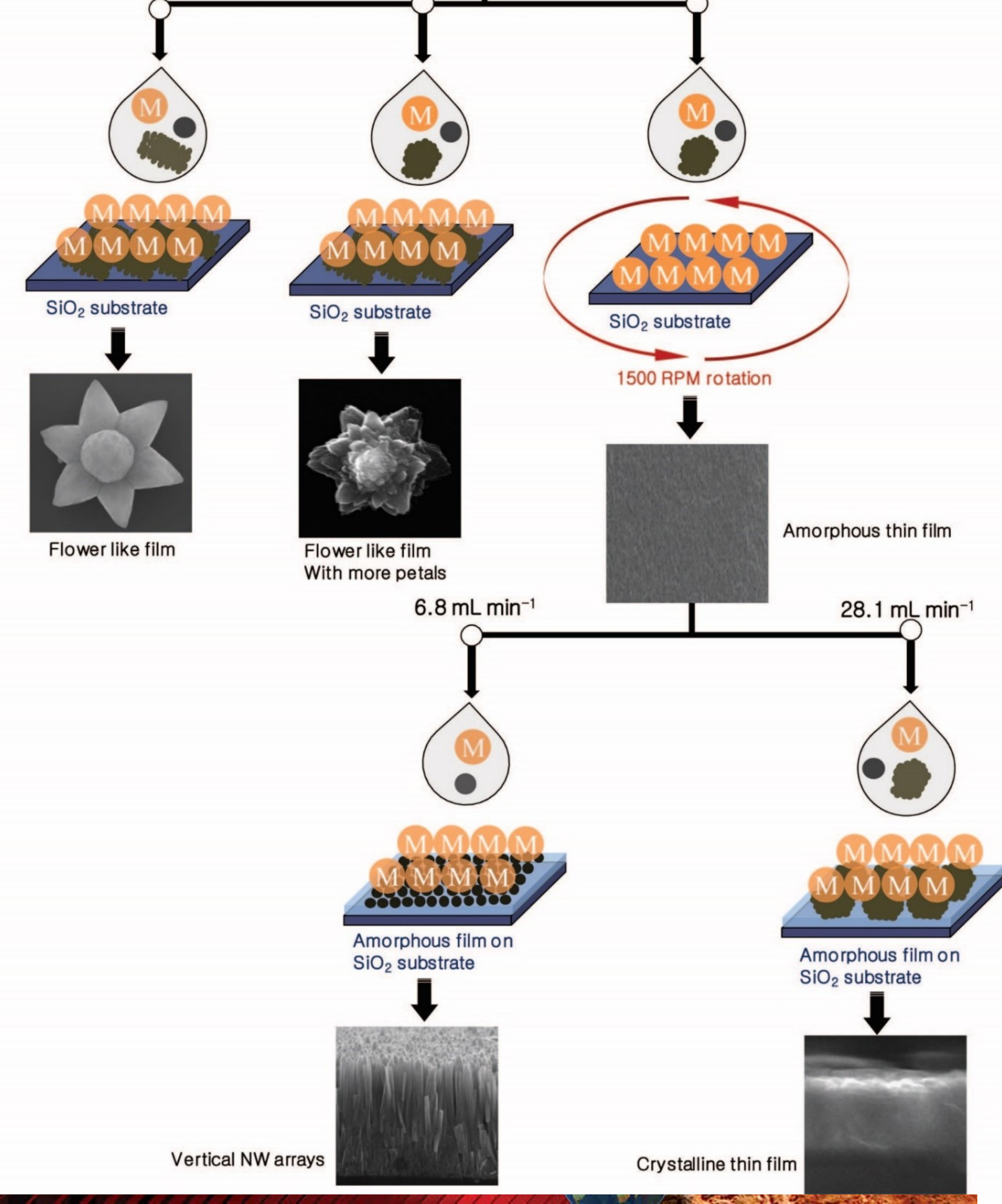
M
SiO_2 substrate
Flower like film
SiO_2 substrate
Flower like film
With more petals
SiO_2 substrate
1500 RPM rotation
Amorphous thin film
6.8 mL min^{-1}
28.1 mL min^{-1}
Amorphous film on
SiO_2 substrate
Amorphous film on
SiO_2 substrate
Vertical NW arrays
Crystalline thin film

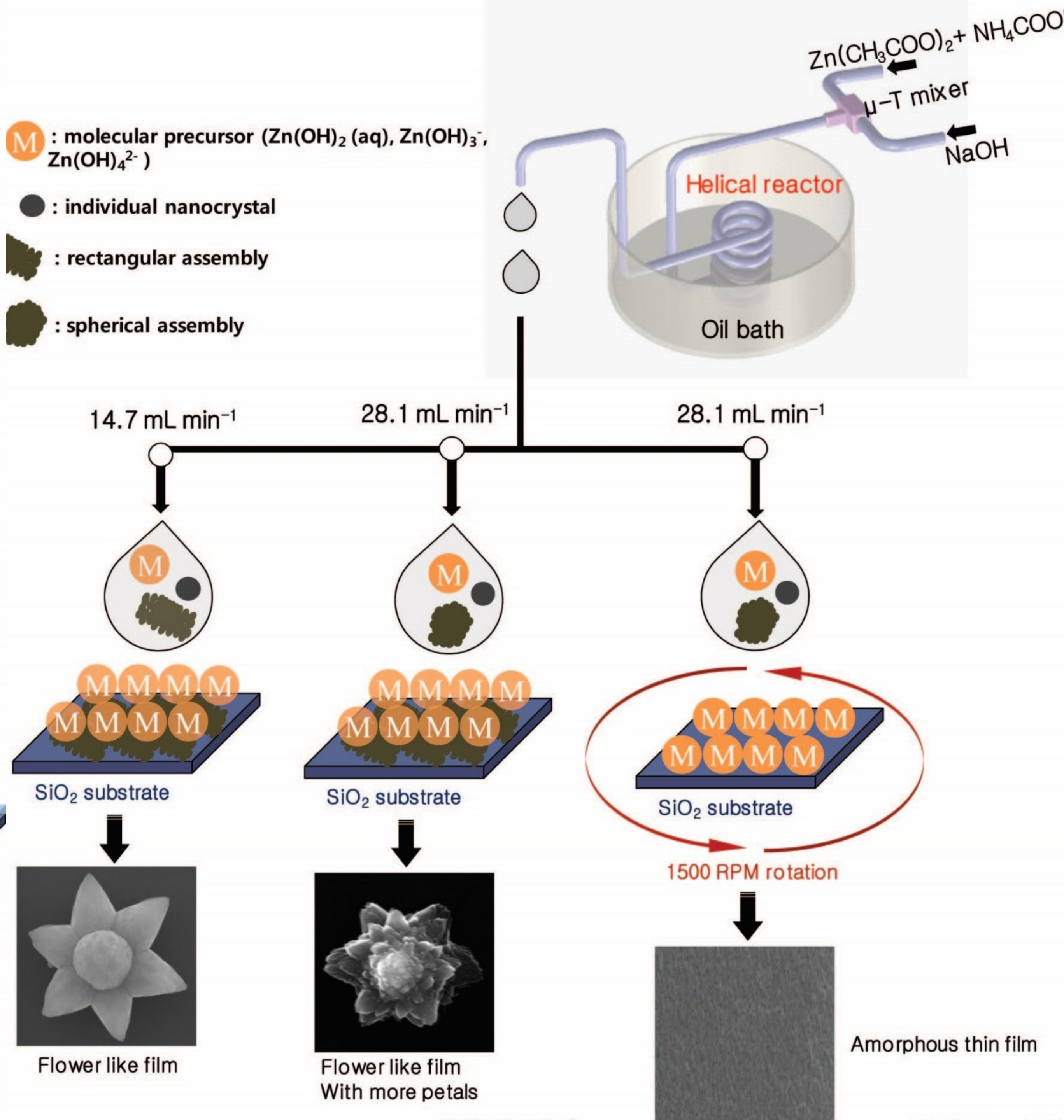
M : molecular precursor ($Zn(OH)_2$ (aq), $Zn(OH)_3^-$, $Zn(OH)_4^{2-}$)
● : individual nanocrystal
: rectangular assembly
: spherical assembly
$Zn(CH_3COO)_2$+ NH_4COO
μ–T mixer
NaOH
Helical reactor
Oil bath
14.7 mL min^{-1}
28.1 mL min^{-1}
28.1 mL min^{-1}
M
SiO_2 substrate
SiO_2 substrate
SiO_2 substrate
1500 RPM rotation
Flower like film
Flower like film
With more petals
Amorphous thin film

Silver Film Fabrication via MAND

Silver mirror reaction

$HCHO+2[Ag(NH3)2]^{+}+2OH^{-} \rightarrow HCOONH4+2Ag+3NH3+H2O$

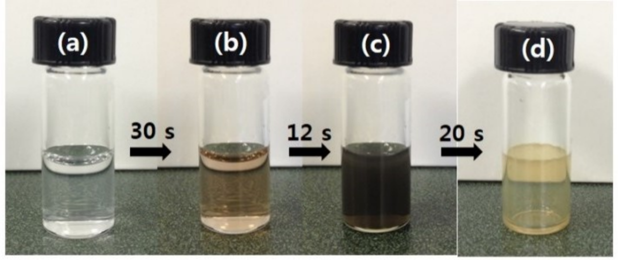

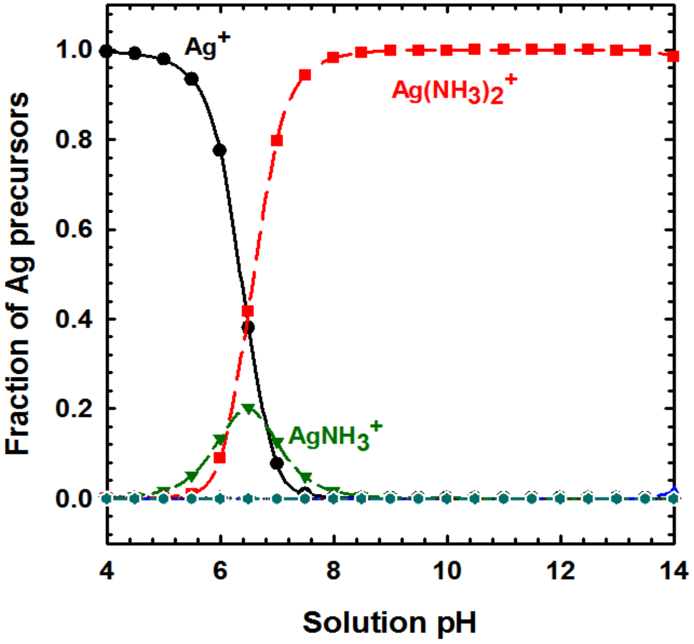

Speciation diagram

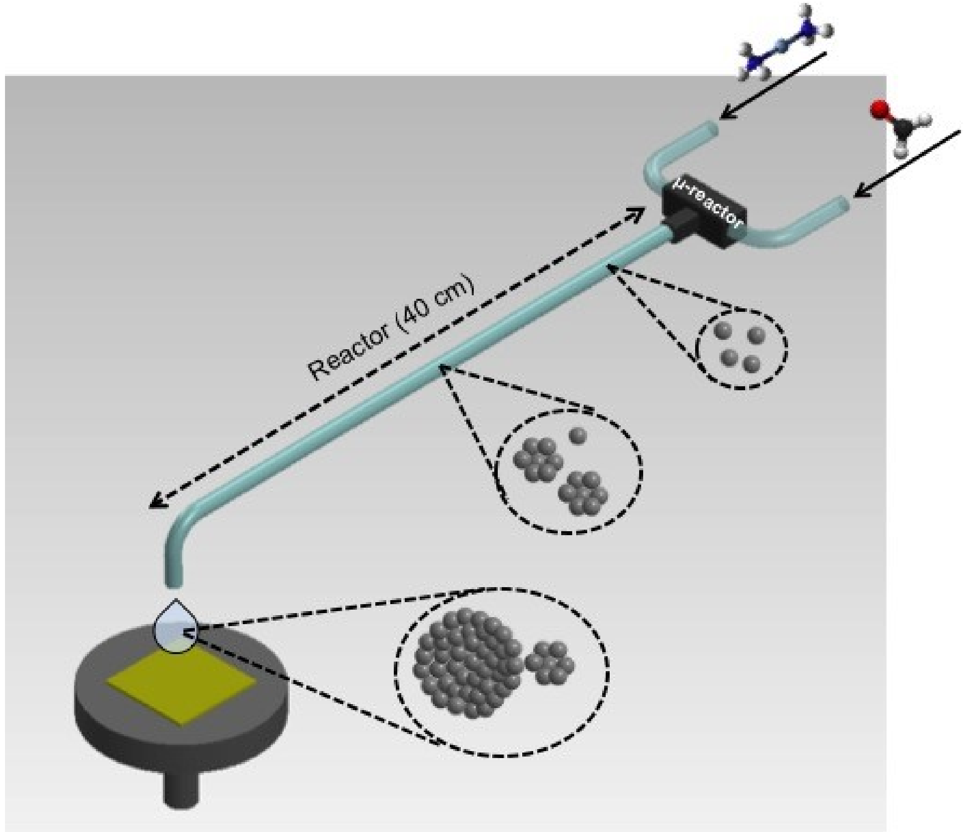

Scheme of MAND to synthesize reactive silver

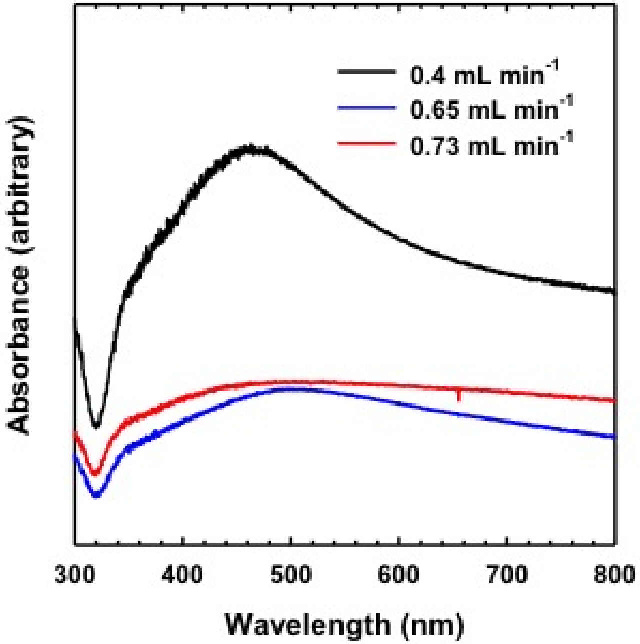

Real time in-situ UV-Vis absorption spectrum

C. Choi, E. Allan-Cole and C. Chang, J. Mater. Chem. C, 2015, DOI: 10.1039/C5TC00947B.

Silver Film Fabrication via MAND at Room Temperature

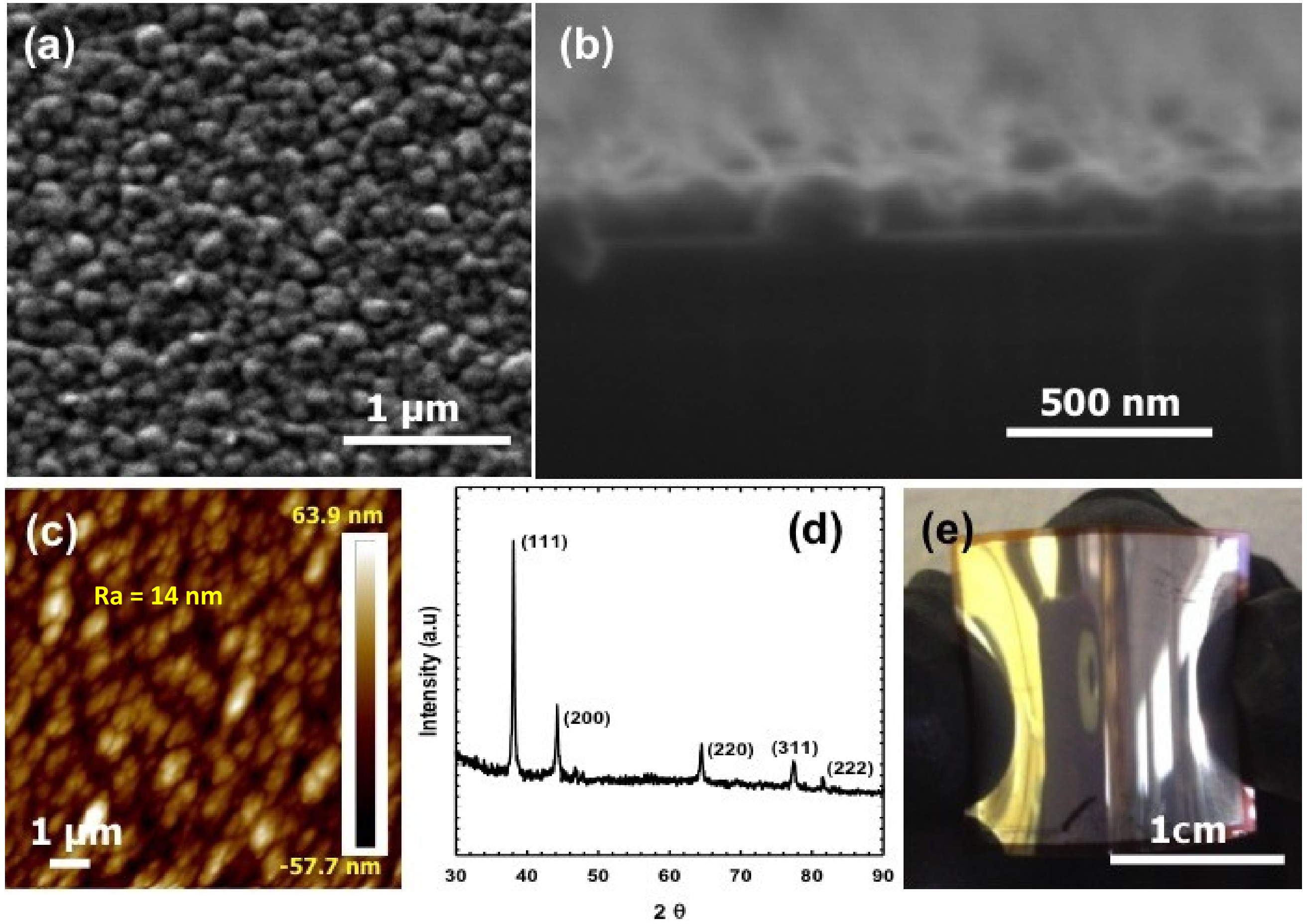

Characterization of reactive silvers

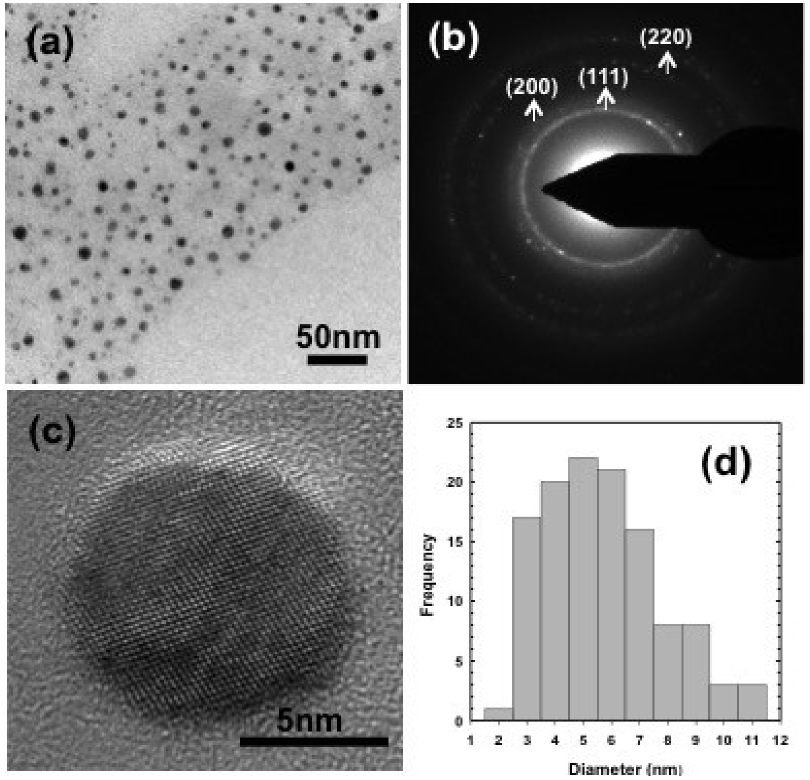

C. Choi, E. Allan-Cole and C. Chang, J. Mater. Chem. C, 2015, DOI: 10.1039/C5TC00947B.

Silver Feature Fabrication via MAND at Room Temperature

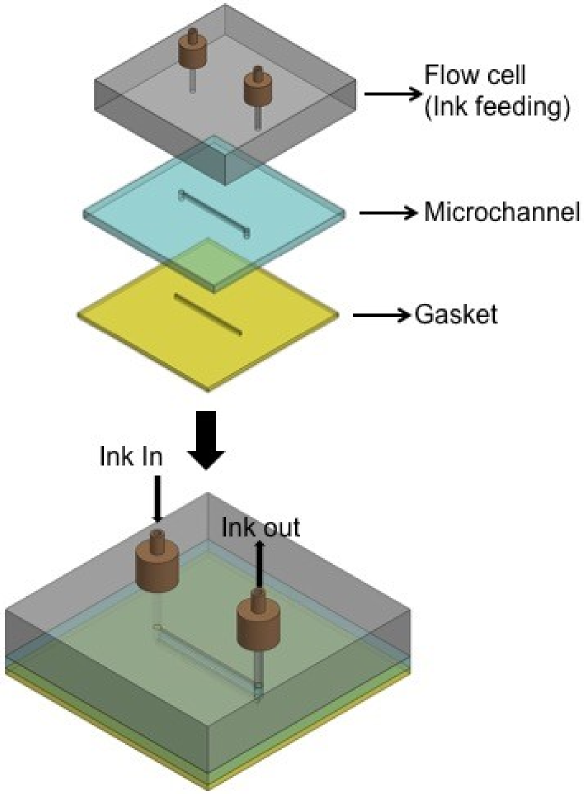

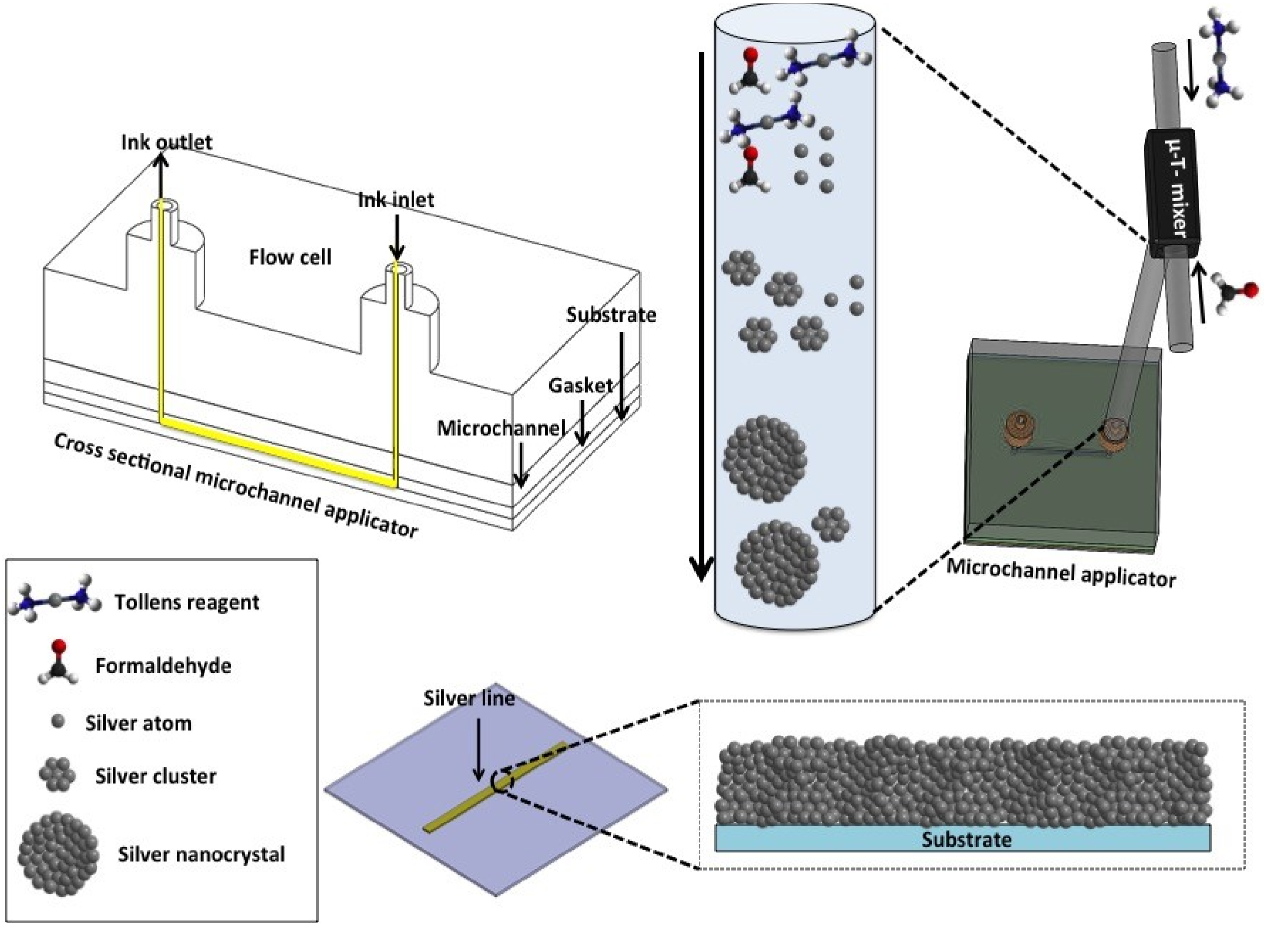

D. Choi, E. Allan-Cole and C. Chang, J. Mater. Chem. C, 2015, DOI: 10.1039/C5TC00947B.

Silver Feature Fabrication via MAND

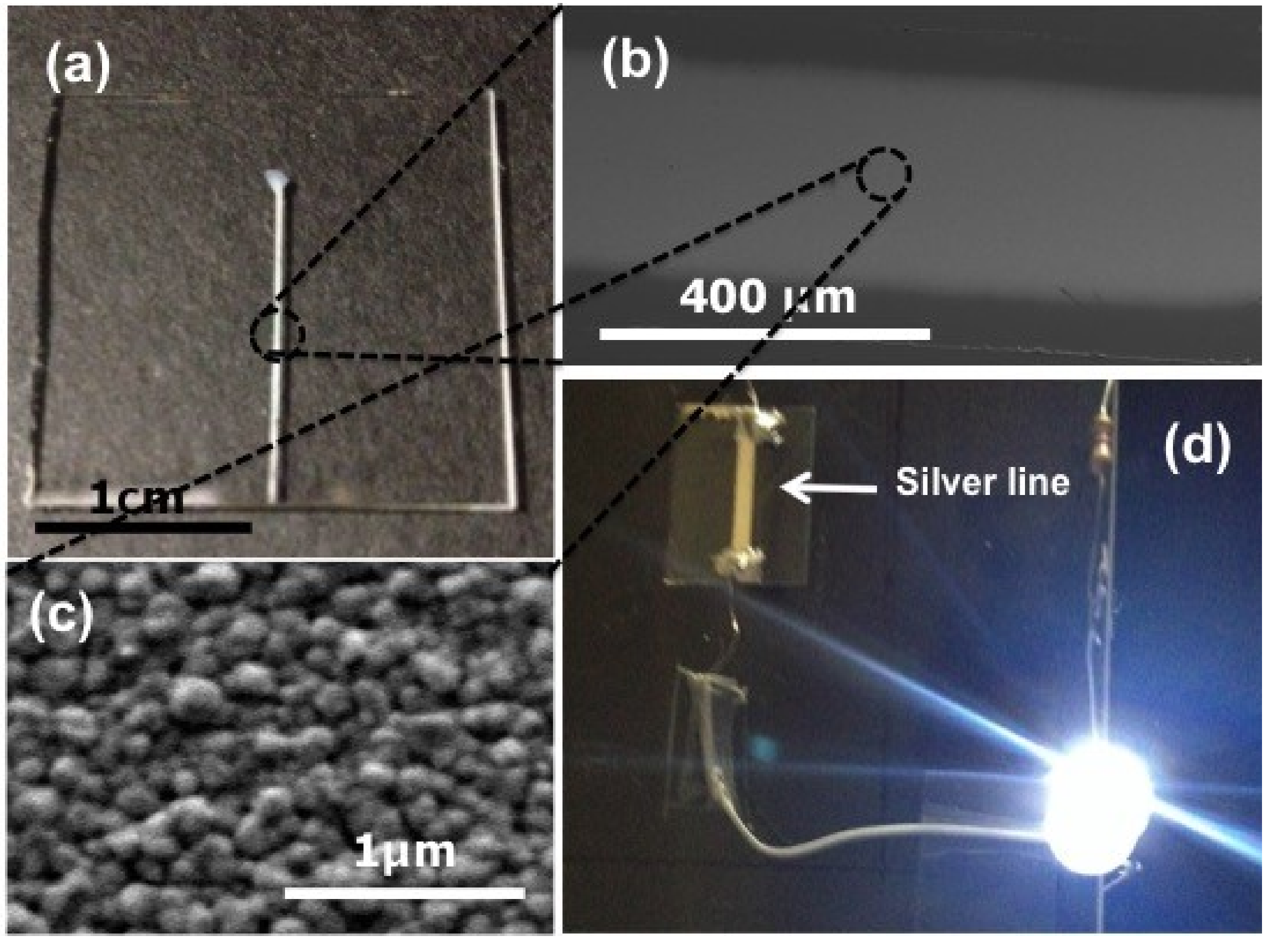

Characterization of silver feature

Electrical conductivity: $1x10^{7}$ S/m

CuO nanorod (left) and CdS fabricated by similar process

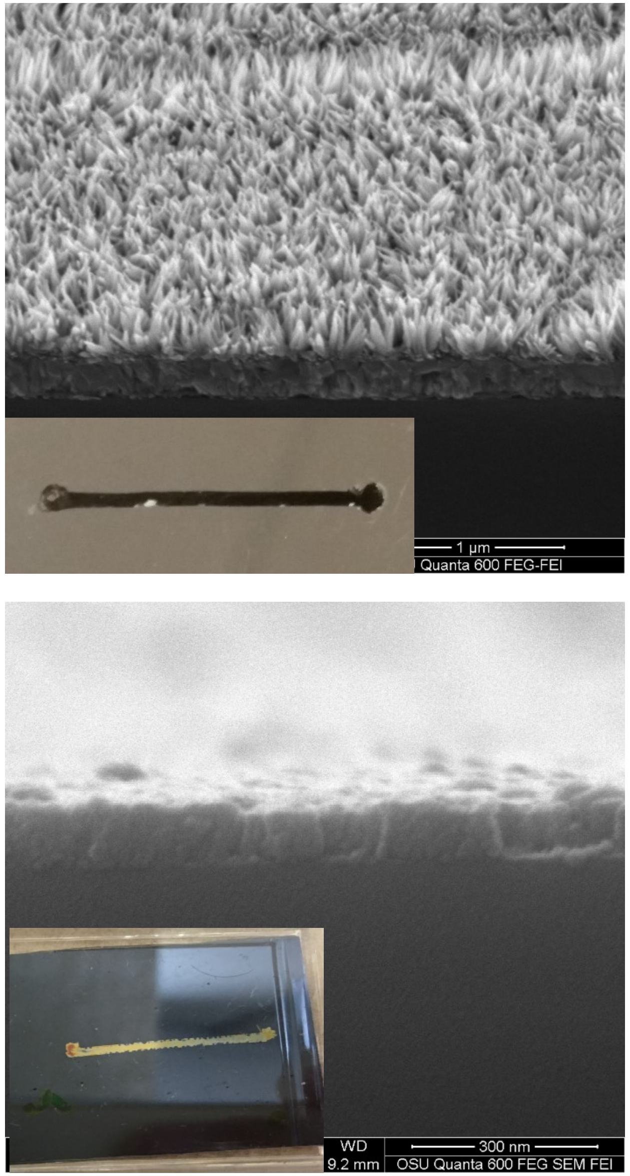

Control by flow rate

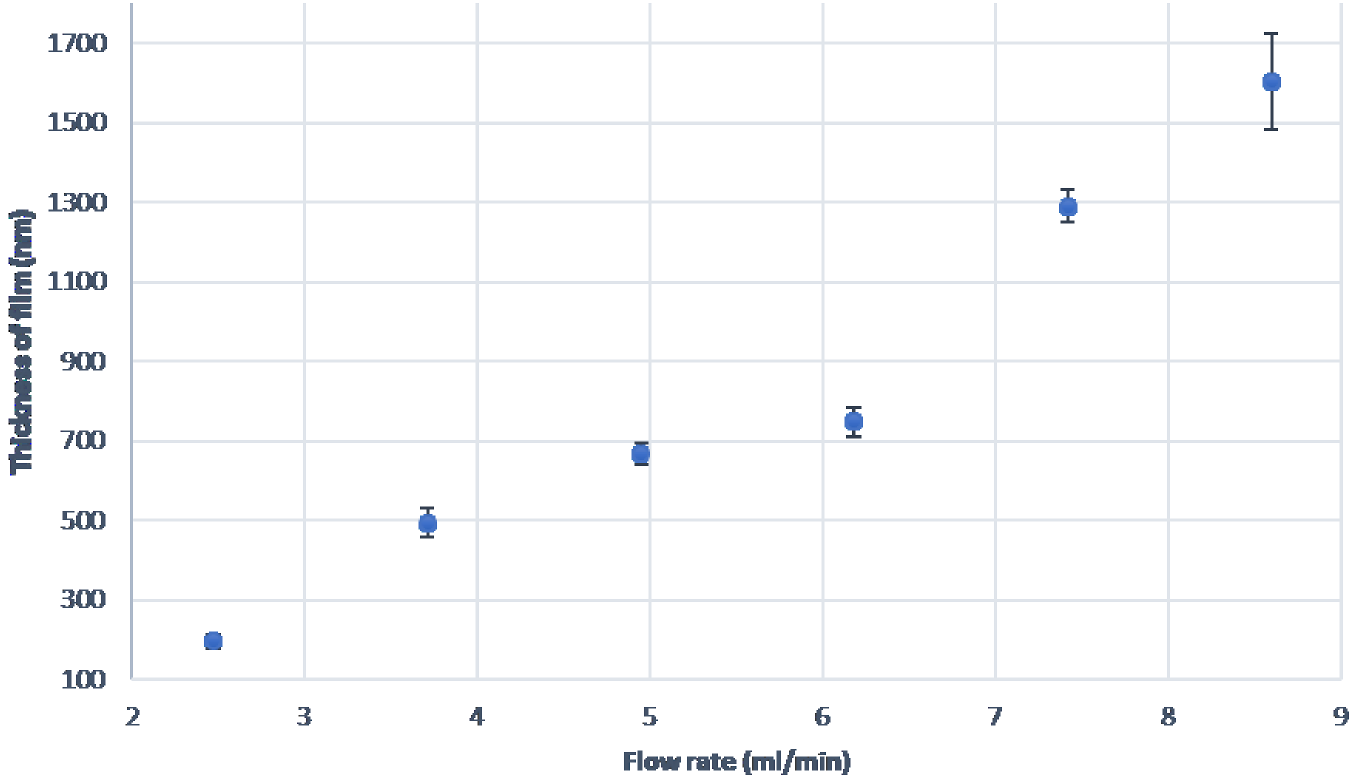

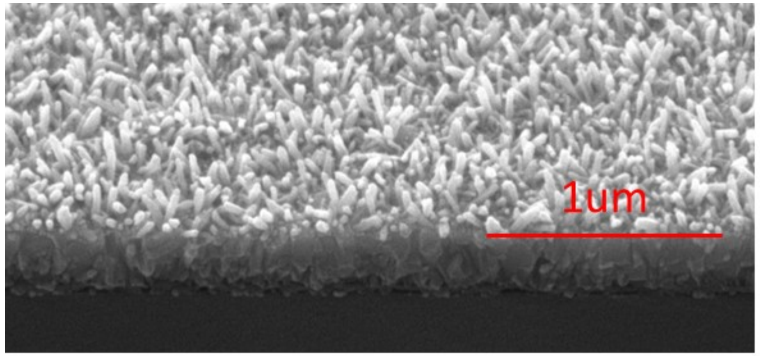

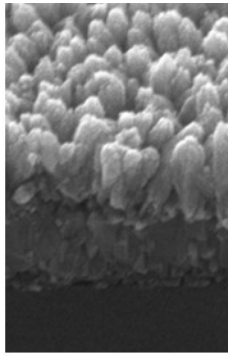

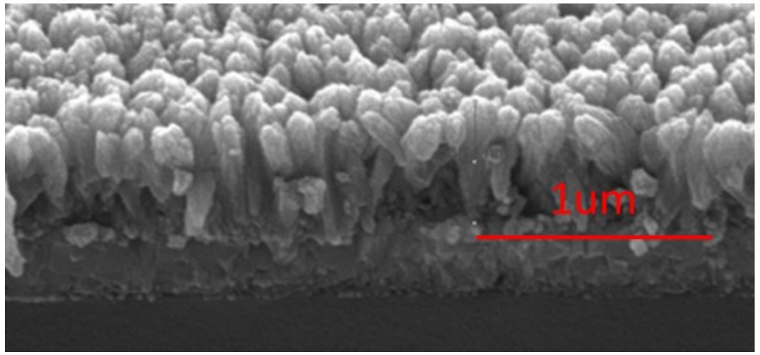

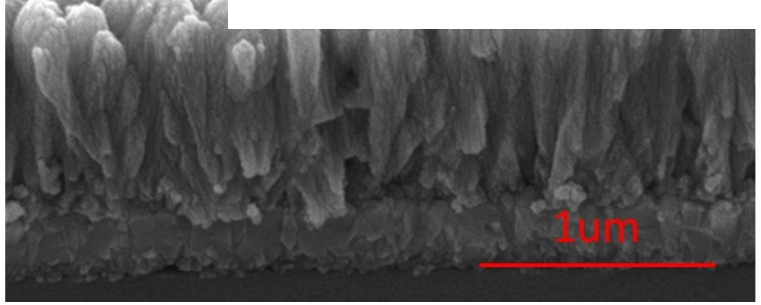

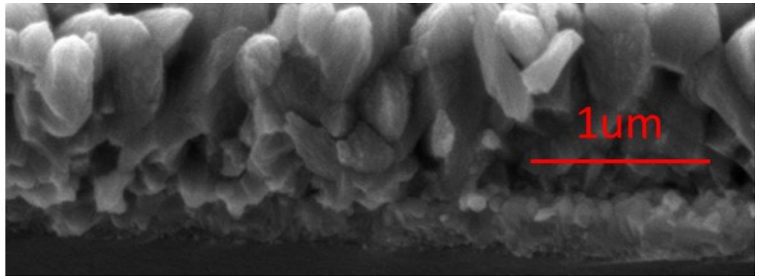

ZnO nanorod formed by combination of MAND and PDMS channel

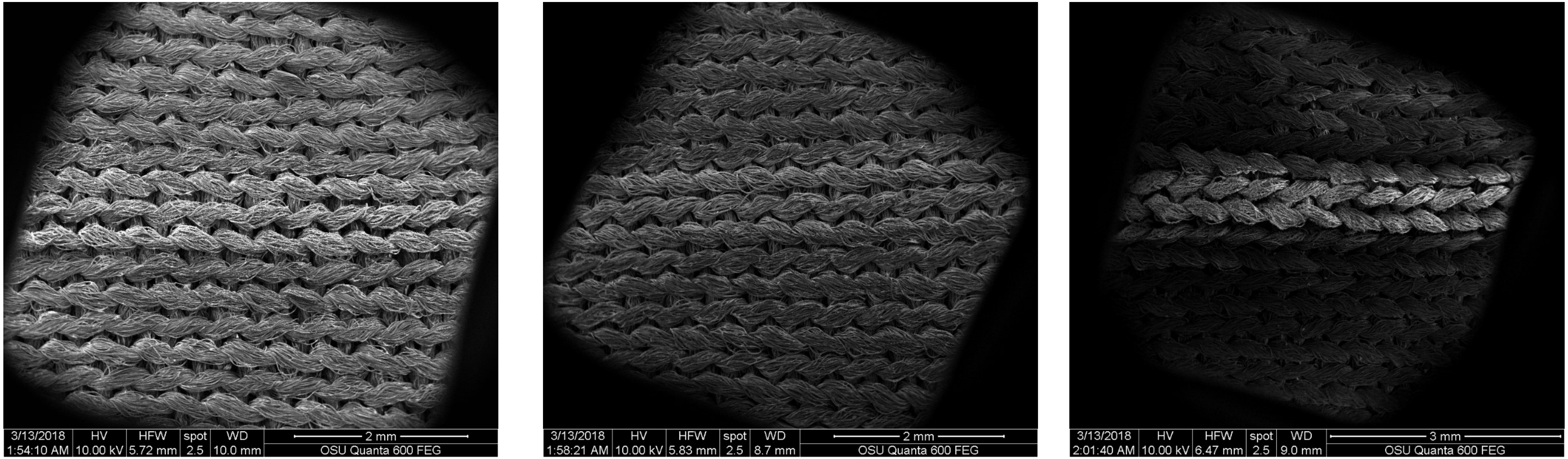

ZnO nanorod formed with different flow rate: from left to right, at 2.56 ml/min, 3.85 ml/min, 5.14 ml/min.

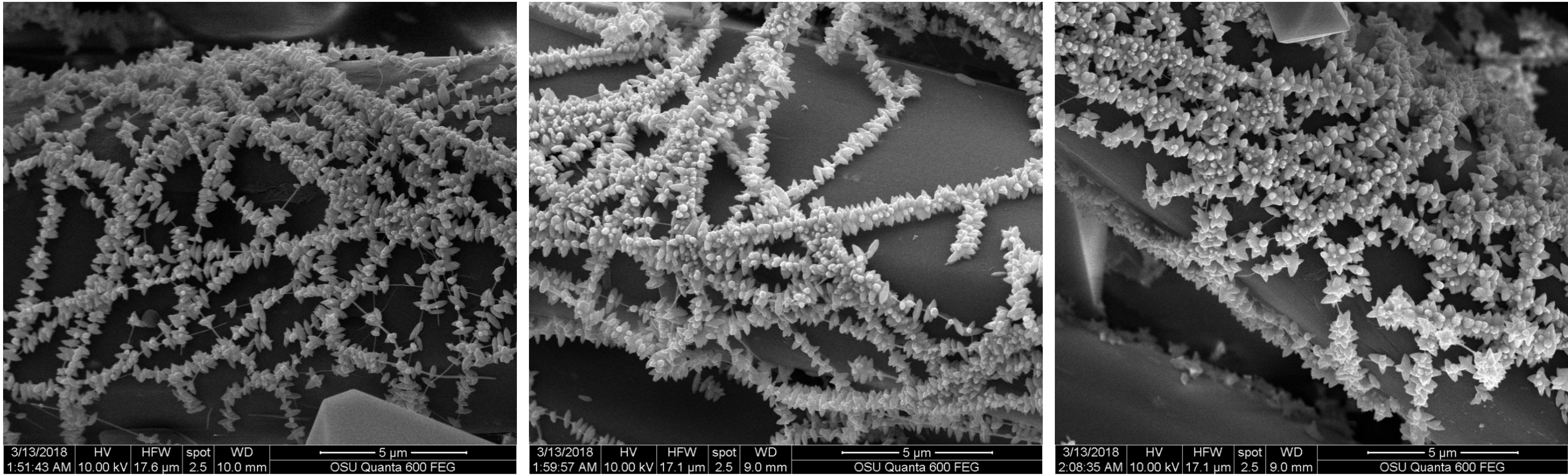

ZnO nanorod formed with different flow rate: from left to right, at 2.56 ml/min, 3.85 ml/min, 5.14 ml/min.

SEM: ZnO nanorods grow on the silver for 10min(with different scales)

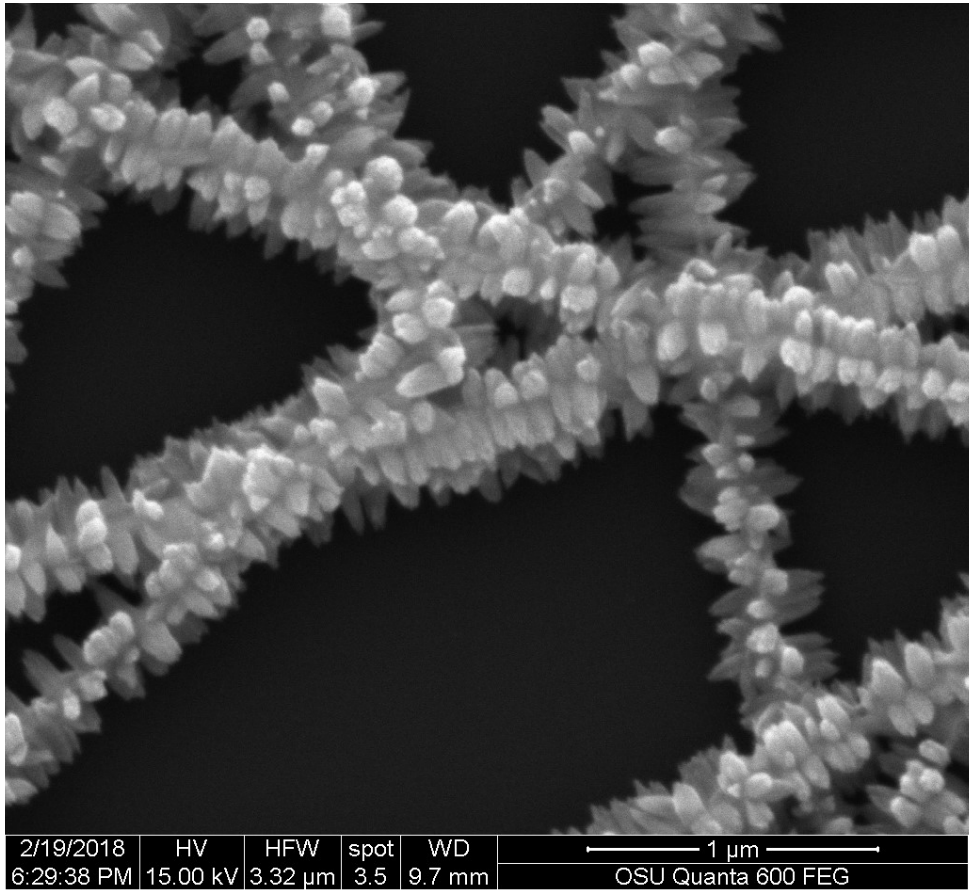

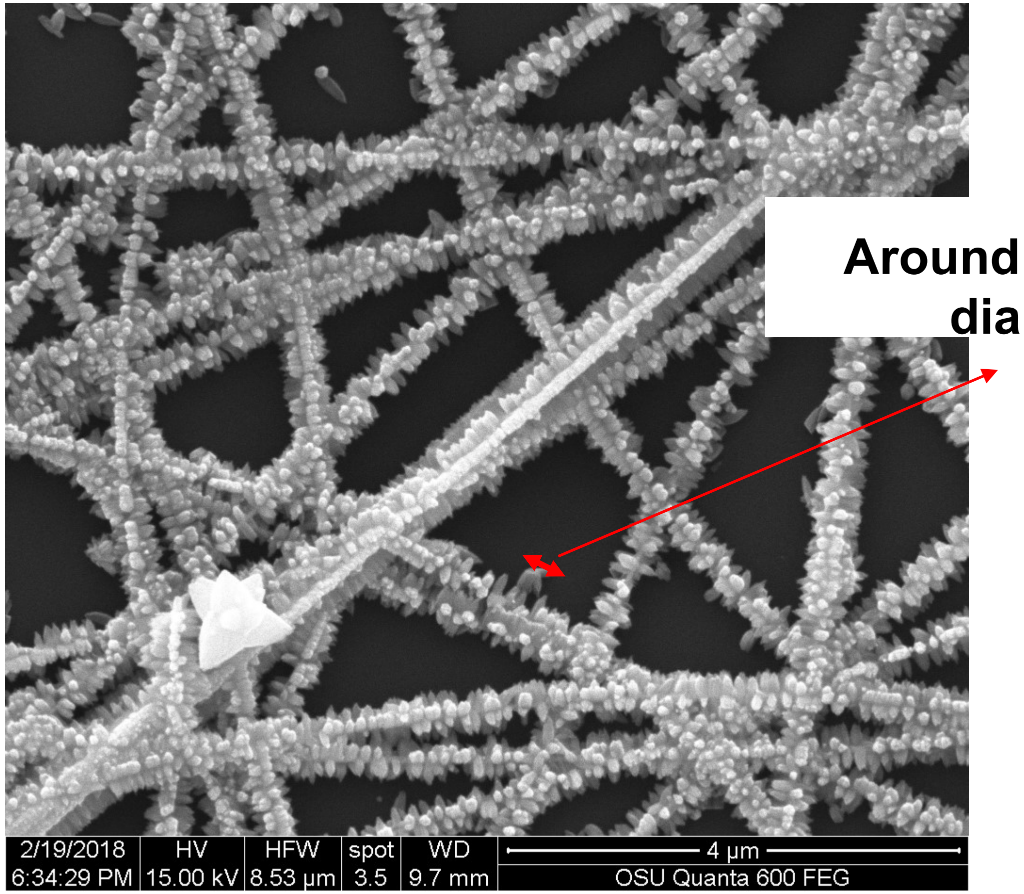

Around 480 nm in diameter

SEM: ZnO nanorods grow on the silver NWs for 20min

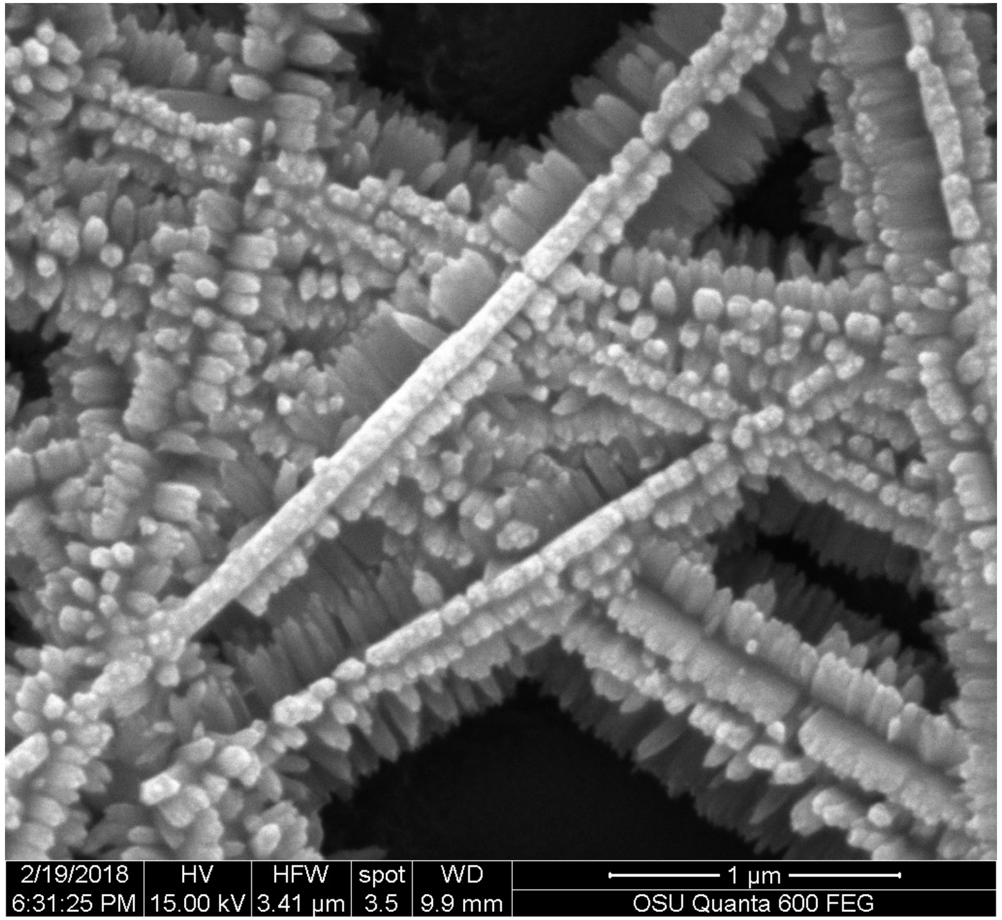

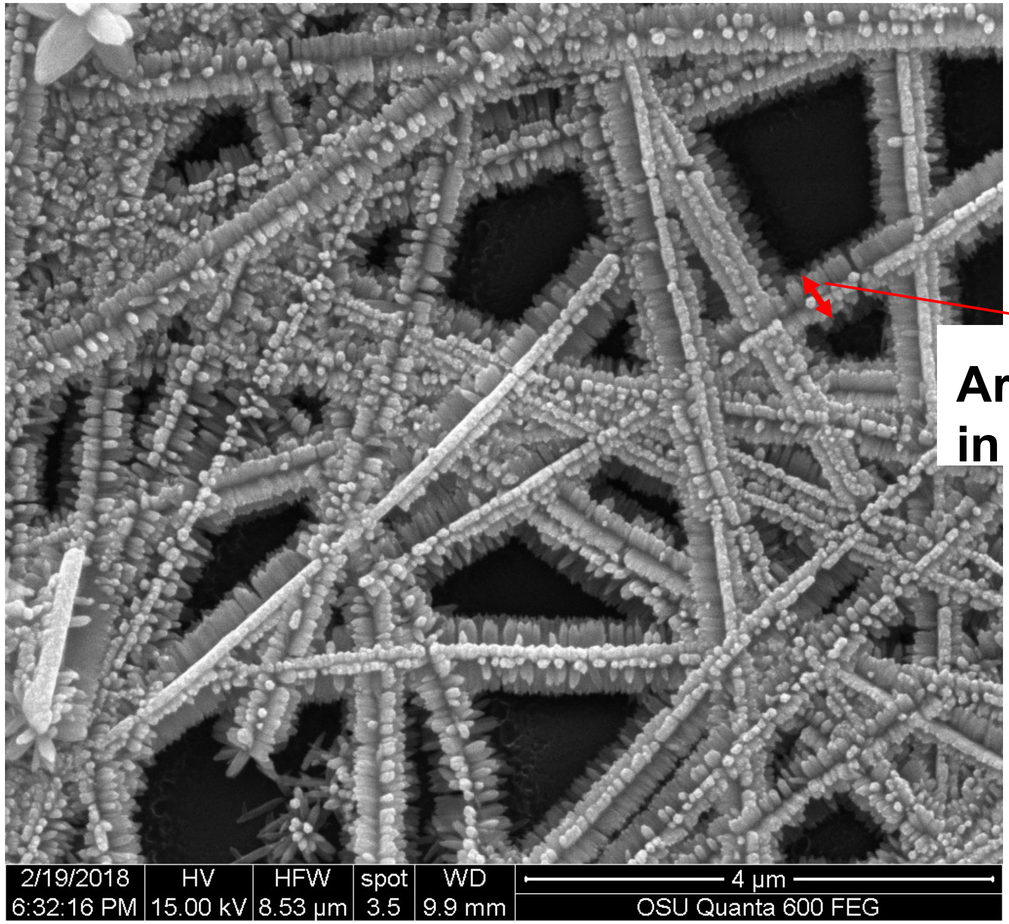

Around 630 nm in diameter

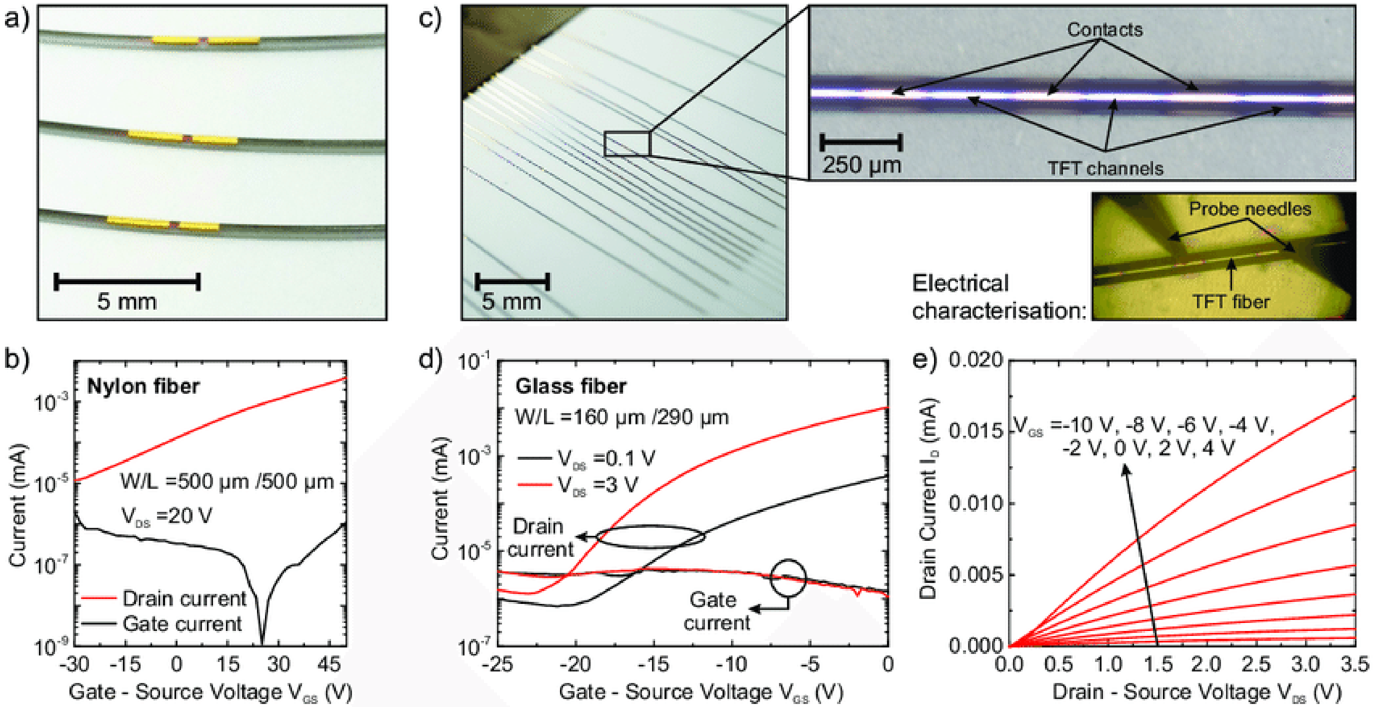

TFTs directly fabricated on fibers: (a) Photograph of TFTs on a 500 µm diameter Nylon fiber fabricated using 1 µm parylene as gate insulator. (b) Corresponding transistor transfer characteristic. (c) Photograph and micrographs of TFTs fabricated on a 125 µm diameter glass fiber fabricated using 100 nm atomic layer deposition (ALD) deposited Al 2 O 3 as gate insulator. Corresponding transfer

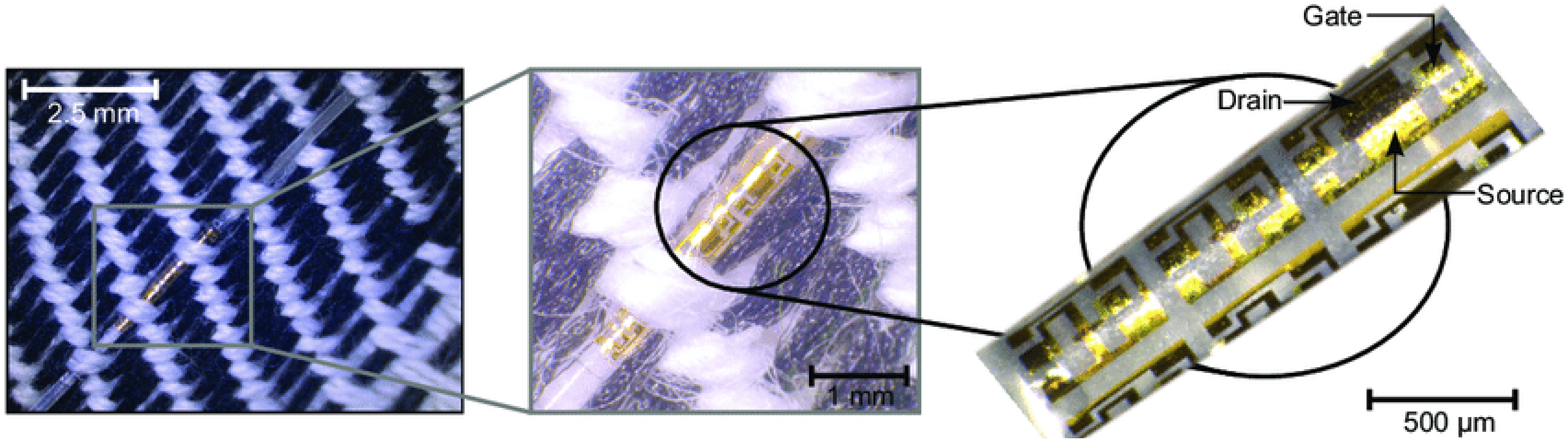

Textile integrated thin-film transistors: IGZO TFTs on Nylon fiber with a diameter of 500 µm are integrated into a commercial textile. The electronic fiber replaces a weft direction cotton yarn.

Niko Münzenrieder et al. Oxide Thin-Film Transistors on Fibers for Smart TextilesTechnologies 2017, 5, 31; doi:10.3390/technologies5020031

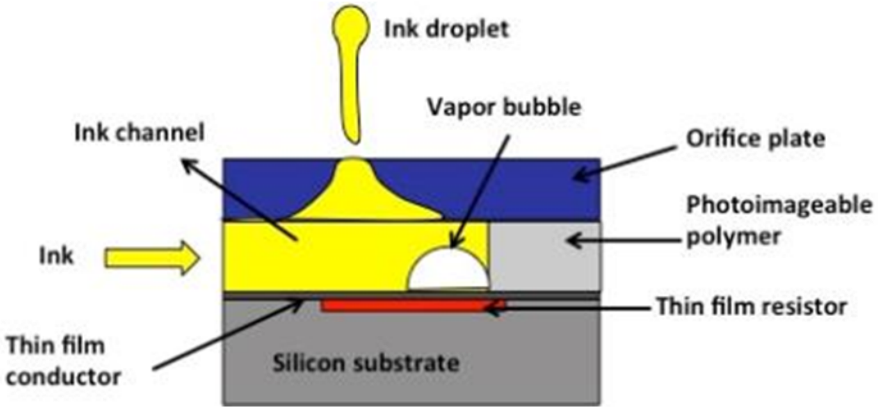

Thermal inkjet printer

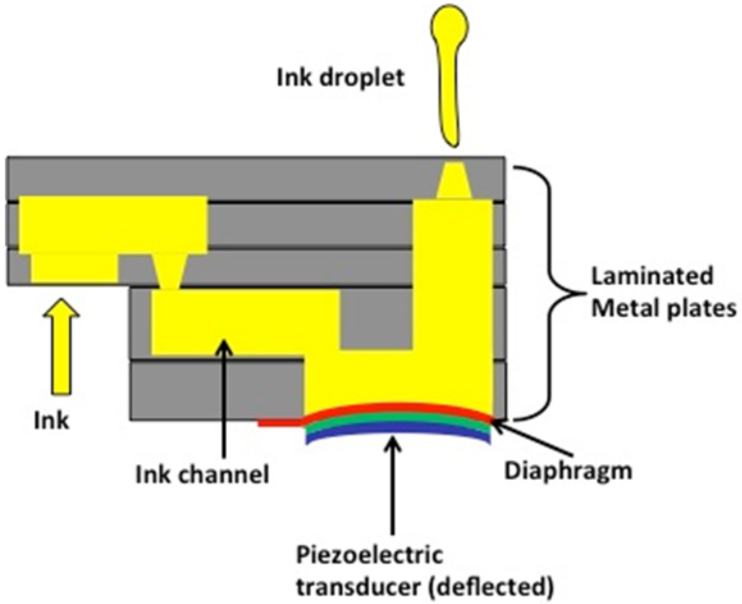

Piezoelectric printer

- Components: ink channel, photoimageable polymer, resistive metallic layer, thin film conductor, orifice plate
- A pulse of electrical current flows through thin film resistor
- Vapor bubble form and eject ink

- Piezoelectric materials used instead of heater
- High electric filed, flowing into the material, deform and squeeze the ink channel and eject ink

C.-H. Choi, L.-Y. Lin, C.-C. Cheng, C.-H. Chang, ECS Journal of Solid State Science and Technology 2015, 4, p3044

Dissolution & Re-crystallization

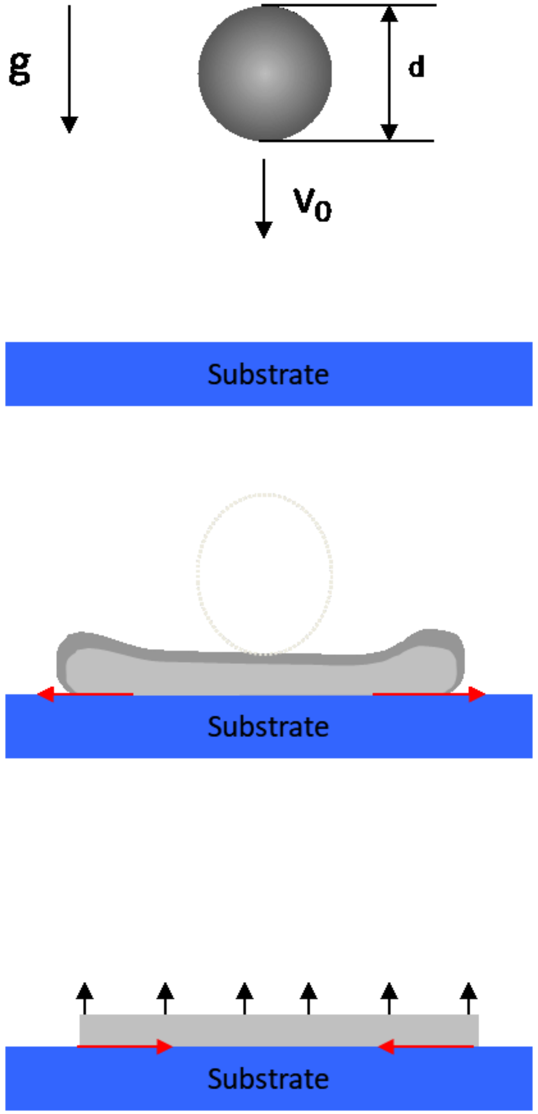

Liquid droplet

Droplet impact and spread

Solvent evaporate and form solid film

Microstructured Salt: NaCl

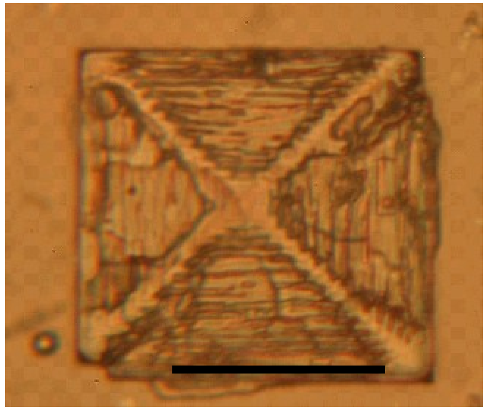

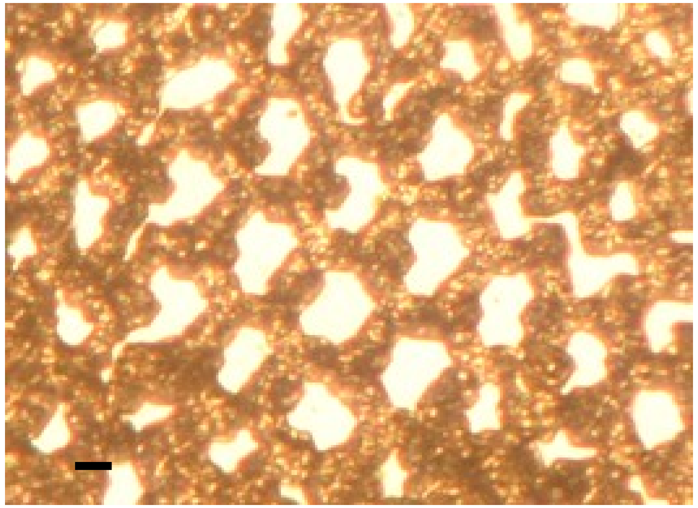

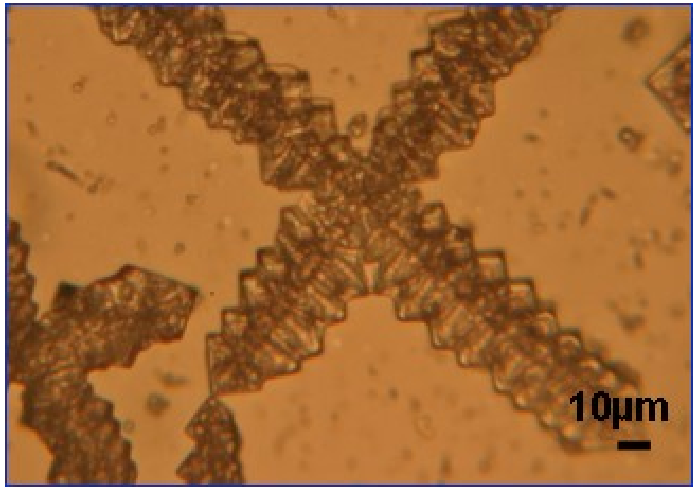

To prepare CuI thin films, commercially available powders of CuI from Alfa-Aesar was dissolved in acetonitrile (CH3CN) at room temperature followed by ultrasonic agitation. The solution was filled into an empty inkjet cartridge and sealed.

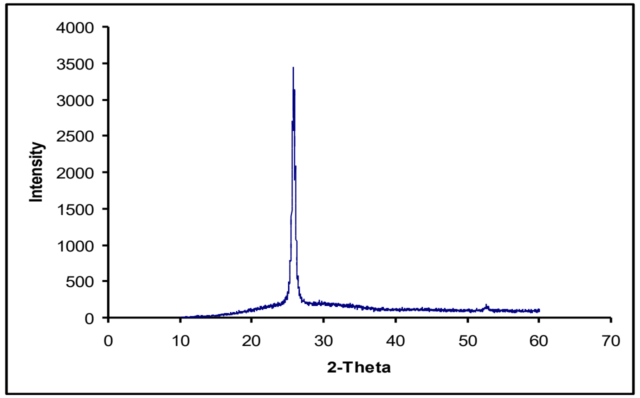

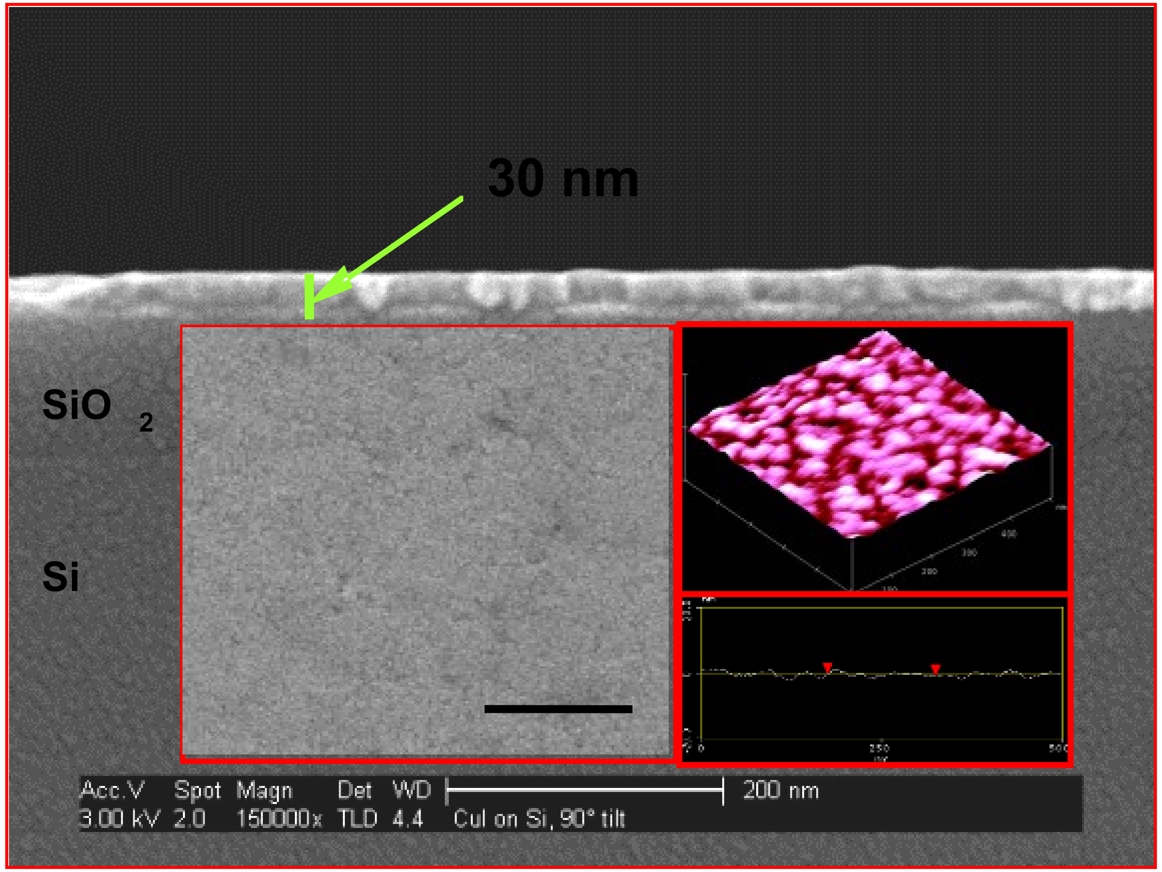

Mechanism of Metal Oxide Thin Film Formation

Metal halide Precursor

Inkjet Printing or Spin

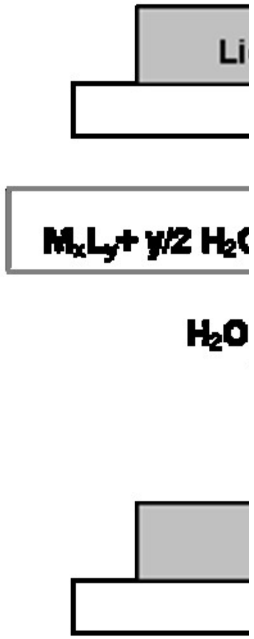

Salt+Water

D. Lee

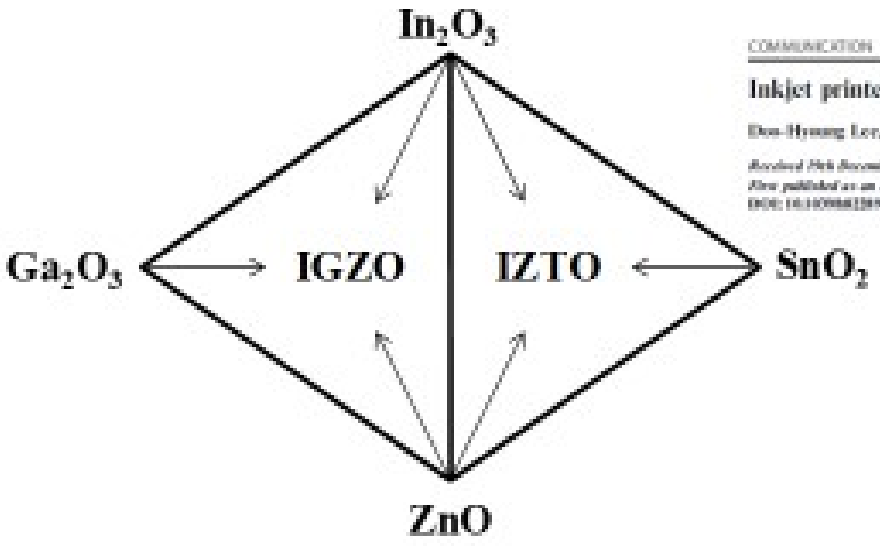

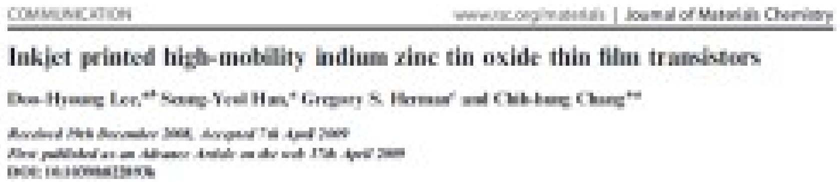
COMMUNICATION www.rsc.org/materials | Journal of Materials Chemistry

Inkjet printed high-mobility indium zinc tin oxide thin film transistors

Doo-Hyoung Lee,*a Sung-Yeol Han,a Gregory S. Herman and Chih-hung Chang*a

Received 19th December 2008, Accepted 7th April 2009
First published as an Advance Article on the web 17th April 2009
DOI: [illegible]

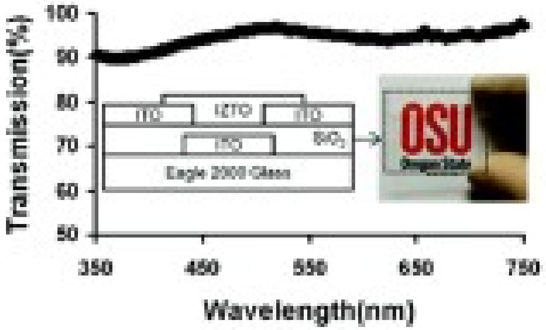

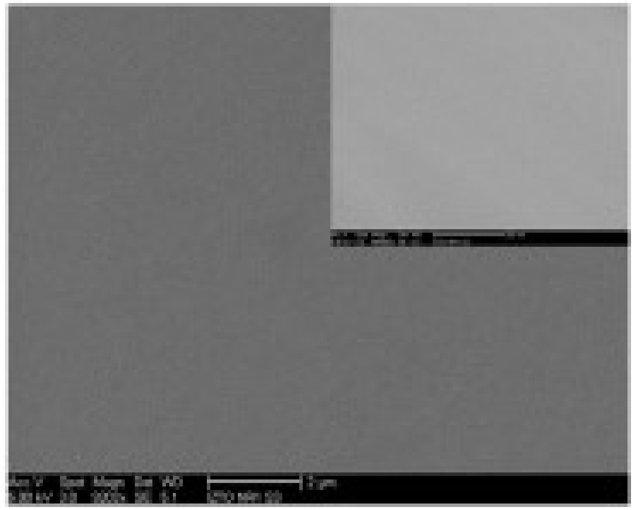

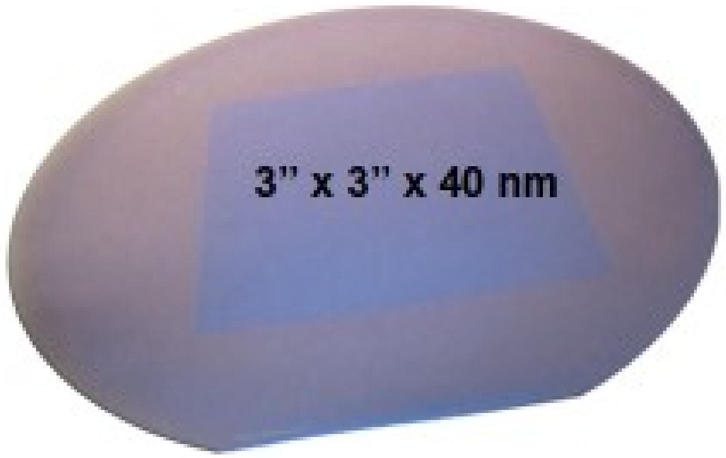

AlOx on moly wire

I. Mo Coated with gold about 50nm thickness
II. Clean with DAI(DI water, Acetone, IPA) and oxygen plasma for 1min
III. Dip coating Moly wire into 1M Al precursor. **2Layer**
IV. 15 min drying at 130C for two layer and 30min annealing(Hot Plate) at 400° C

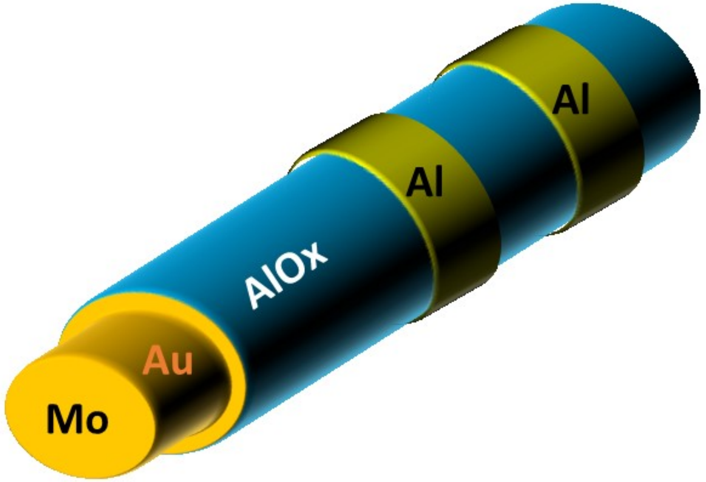

Structure diagram for the fabrication AlOx layers on Mo wire by dip coating method

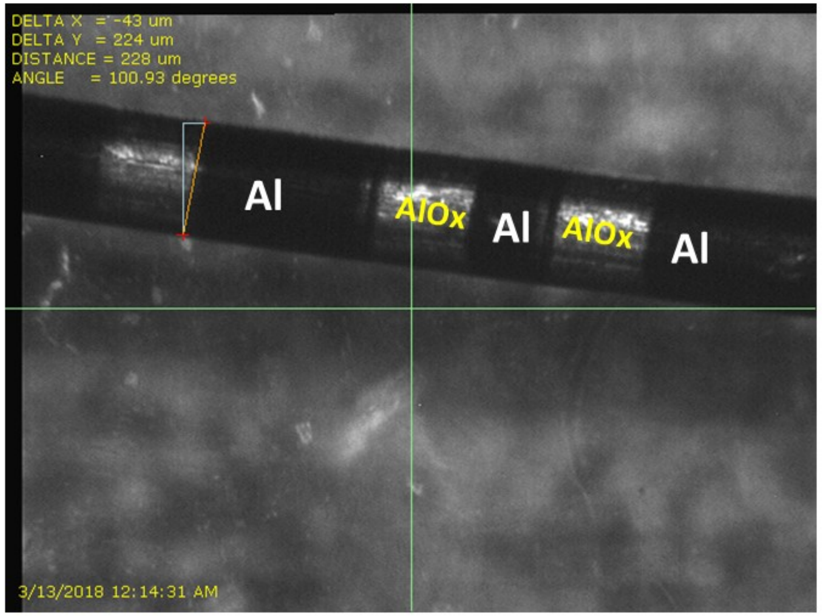

Image under the camera

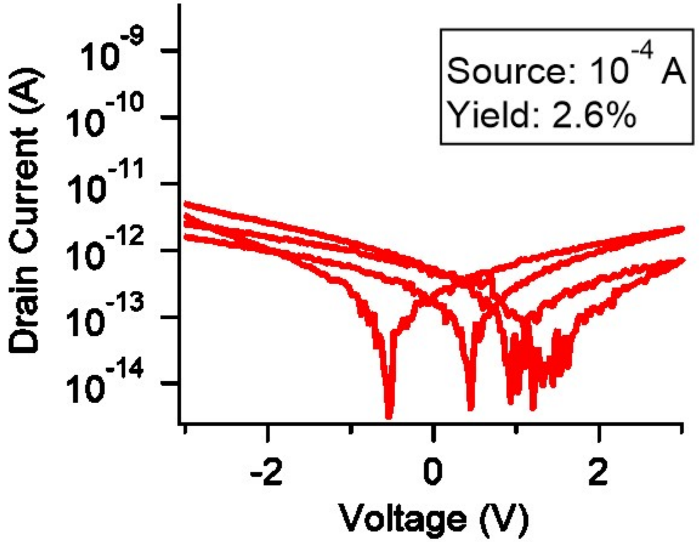

Insulation Properties of dip coated AlOx

Inkjet Printed Y_AlOx on moly wire

I. Clean with DAI(DI water, Acetone, IPA) and oxygen plasma for 5 min
II. Inkjet printed 3-4 layer 20% Y_AlOx on the Mo wire
III. Dry and anneal it (Oven) at 400° C for 30 min
IV. Use Copper wire as metal to test the insulation proerties

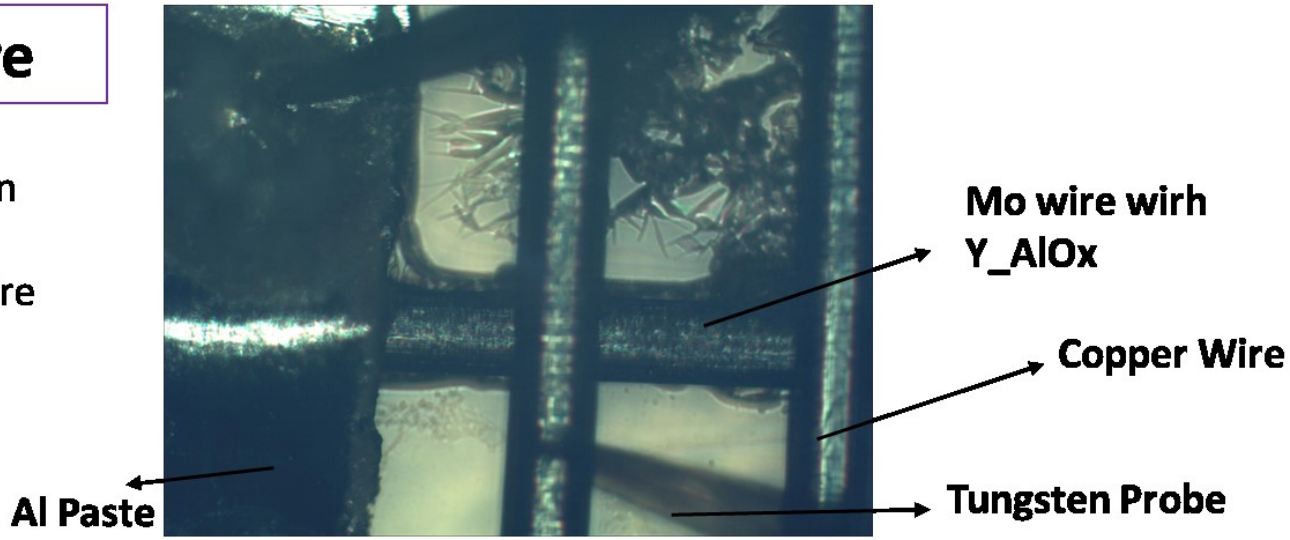

Image under the camera

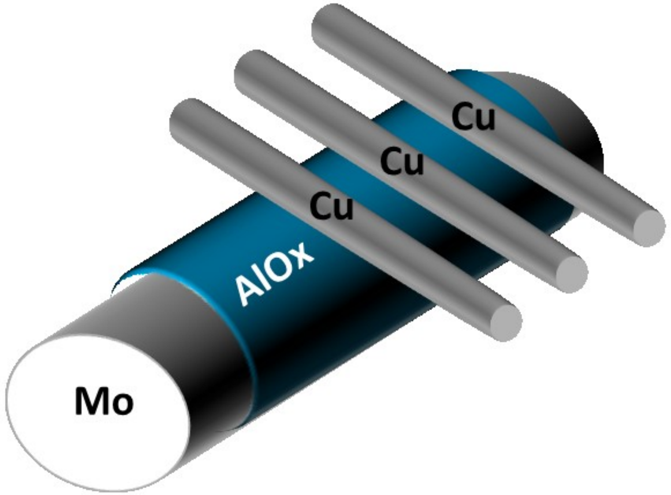

Structure diagram for the fabrication AlOx layers on Mo wire By Inkjet Print

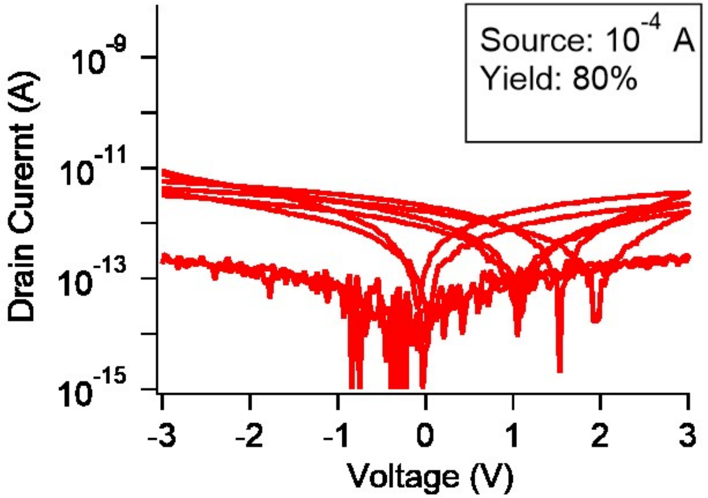

Insulation Properties of Inkjet Printed AlOx

Inkjet Print YVO_4 on moly wire

I. YVO_4 Nanoparticle
II. Dissolve in DI water up to 5ml
III. Filter it with 0.2um PTFE filter

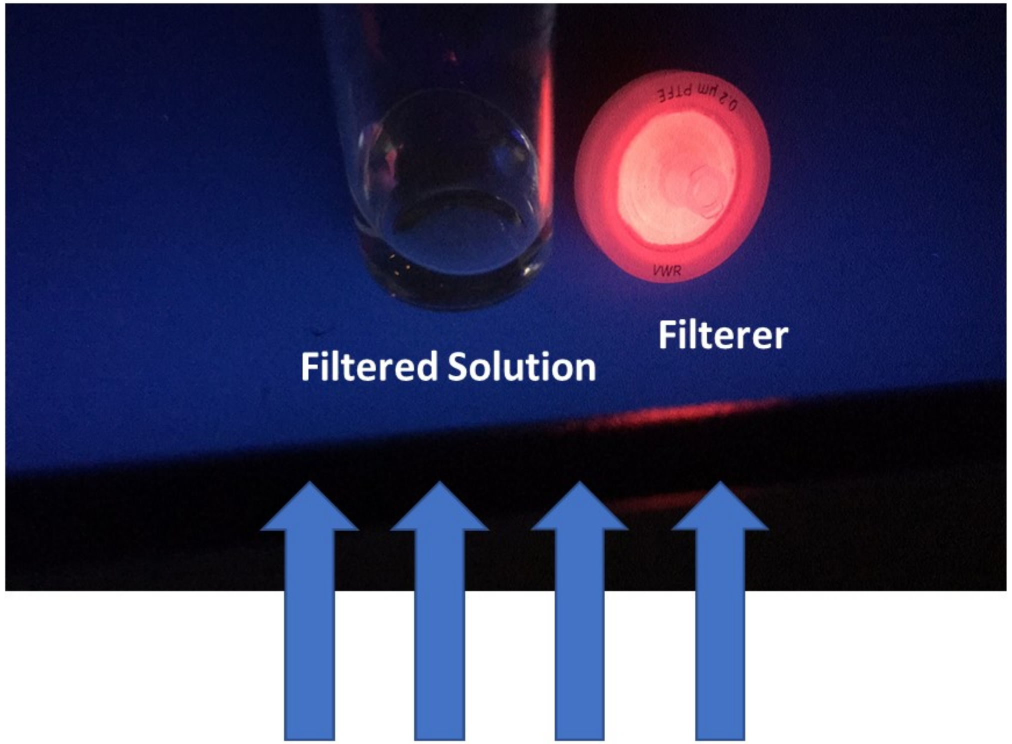

UV light Source

Smaller size was chosen

UV light Source

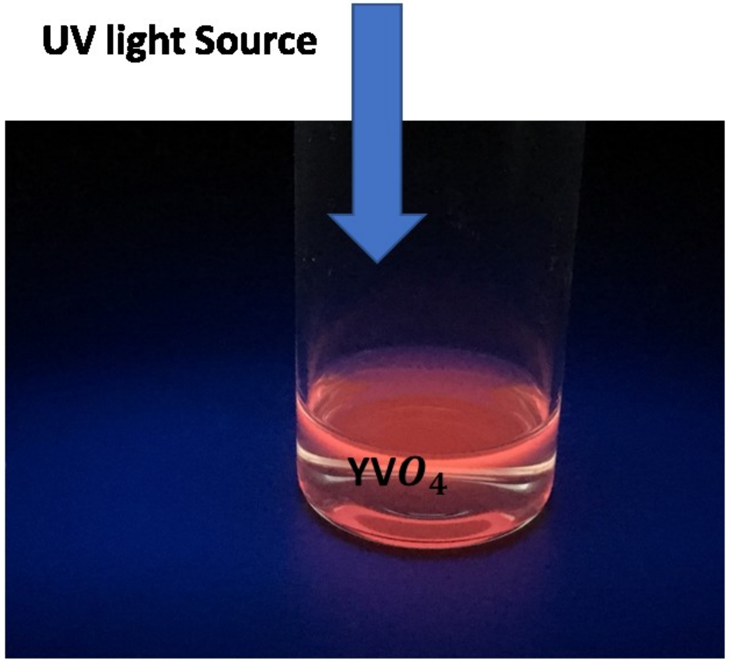

256nm
UV light Source

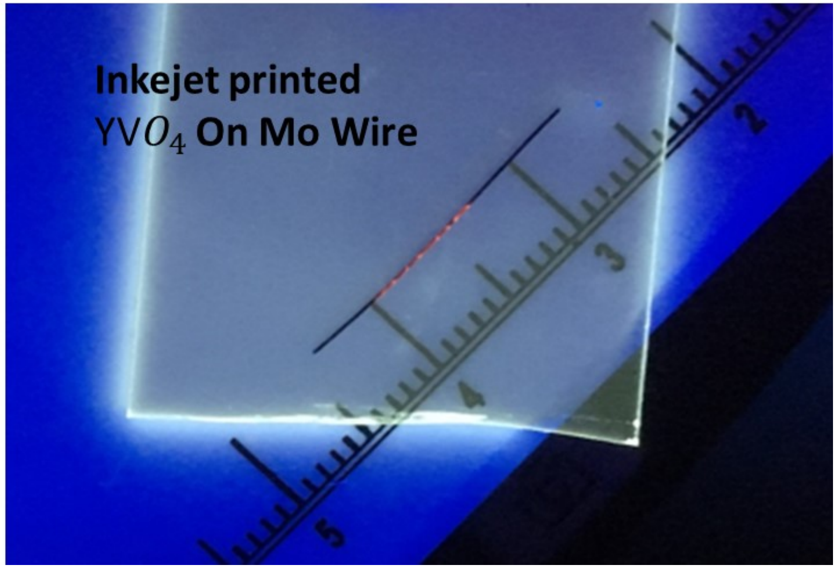

Inkjet Print Indium Oxide on moly wire

Element	Wt %	At %
O K	10.65	42.36
MoL	74.40	49.35
InL	14.96	8.29
Total	100.00	100.00

Element	Wt %	At %
O K	11.80	45.34
MoL	70.34	45.09
InL	17.86	9.57
Total	100.00	100.00

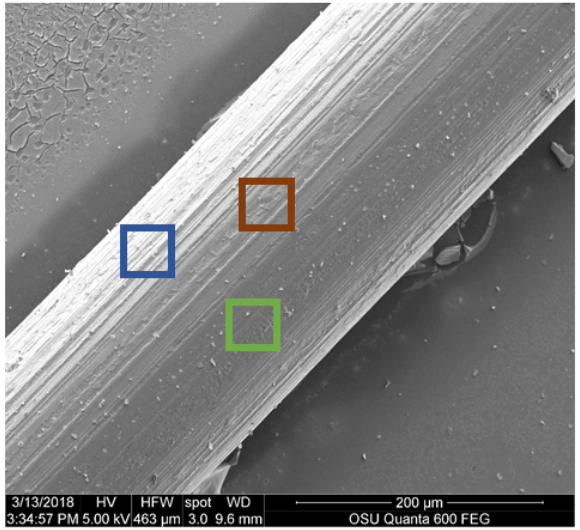

Element	Wt %	At %
O K	14.66	52.63
MoL	47.68	28.54
InL	37.65	18.83
Total	100.00	100.00

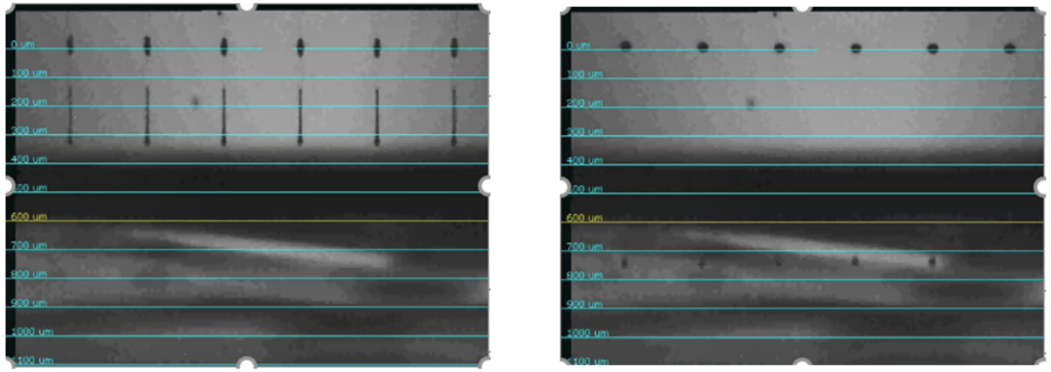

Easy to print wit stable droplet and high velocity

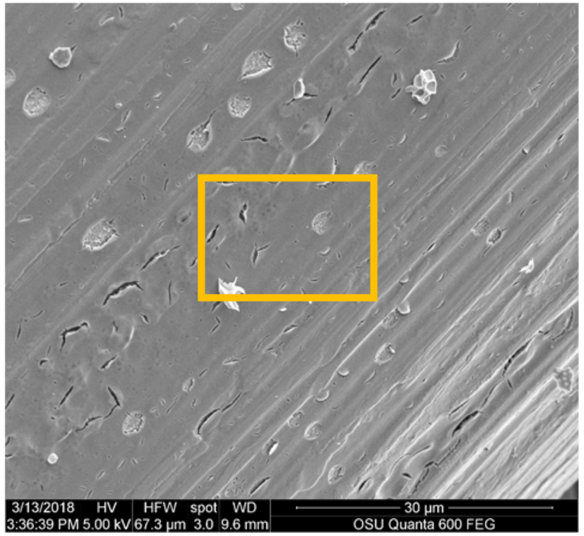

Element	Wt %	At %
O K	22.10	67.06
InL	77.90	32.94
Total	100.00	100.00

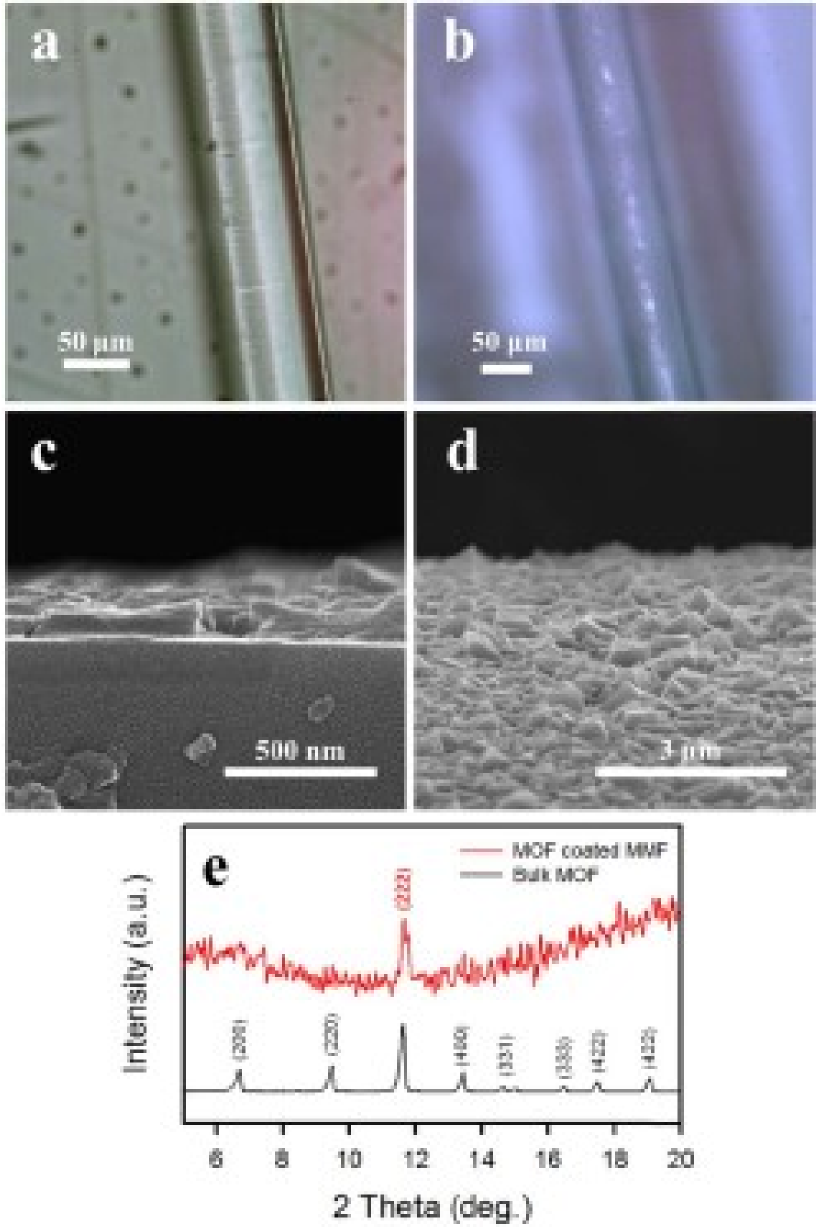

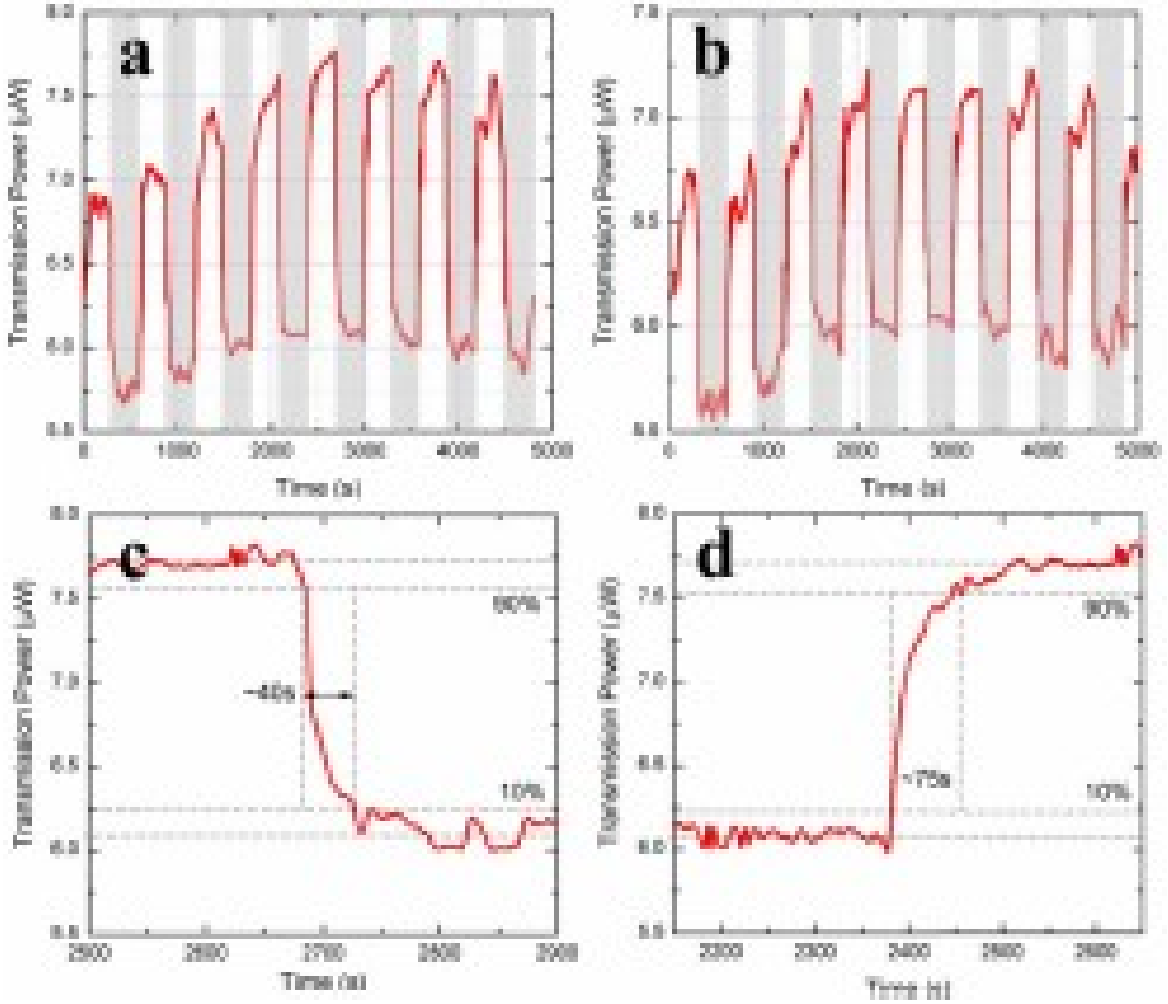

Real-time response of the fiber-optic sensor to alternating Ar and CO2 flows at (a) 1572.5 nm, (b) 1500 nm; Response time of the fiber-optic sensor for (c) absorbing and (d) desorbing CO2.

Ultrashort Near-Infrared Fiber-Optic Sensors for Carbon Dioxide Detection Xinyuan Chong, Ki-Joong Kim, Paul R. Ohodnicki, Erwen Li,Chih-Hung Chang, and Alan X. Wang. IEEE SENSORS JOURNAL, VOL. 15, NO. 9, 2015

Acknowledgement

This work is supported by the

- Walmart Manufacturing Innovation Fund
- NSF Scalable Nanomanufacturing
- DOE ITP Program
- ONAMI
- Oregon BEST
- AUO